Investigation of the Likelihood of Green Infrastructure (GI) Enhancement along Linear Waterways or on Derelict Sites (DS) Using Machine Learning.

Author: S.M. Labib

School of Environment, Education and Development (SEED), University of Manchester, Arthur Lewis building (1st Floor); Oxford Road; Manchester; M13 9PL. Email: sm.labib@manchester.ac.uk

Abstract:

Studies evaluating potential of Green Infrastructure (GI) development using traditional Boolean logic-based multi-criteria analysis methods are not capable of predicting future GI development under dynamic urban scape. This study evaluated robust soft-computing-based methods of artificial intelligence (Artificial Neural Network, Adaptive Neuro-Fuzzy Interface-System) and used statistical modelling (logistic regression) to predict GI or grey transformation likelihoods for vacant sites along waterway corridors (WWC) and derelict sites (DS) based on ecological, environmental, and social criteria. The study found that the ANN and ANFIS models had better predictive capacity and more accuracy (72% accurate) than logistic models (65% accurate). Site sizes, population coverage, and air pollution were identified as the main influencing factors regarding GI/GY transformation. Finally, for Manchester, the likelihood of GI transformation was higher for WWCs (80%) than for DS (60%), and DS were more likely to transform into GY based on current trends.

Key words: *Green Infrastructure; Derelict Sites; Ecological Corridors; Machine learning; Urban Planning*

1. Introduction

Green Infrastructure (GI) is an emerging research topic in the domains of urban planning, ecosystem management, and climate change (Mell, 2016; Benedict and McMahon, 2012; Tzoulas et al., 2007). Due to urbanization, it is projected that by 2050, 66% of the global population (5 billion people) will live in urban areas, and urban (Grey) infrastructure (GY) expansion will increase at nearly twice the rate of urban population growth (Güneralp and Seto, 2013). While there are economic and social benefits associated with urbanization, the phenomenon also causes loss of habitat and biodiversity (McDonald et al., 2008; McKinney, 2002), increased pollution, negative effects on health and wellbeing, and increased climate change vulnerability (Sinnett et al., 2015; Gill et al., 2007). GI can be used to remediate problems induced by rapid urbanization. GI's ability to create and conserve habitat, promote biodiversity, reduce pollution, increase health and wellbeing among citizens, and increase climate change resilience (Nielsen et al., 2017; Mell, 2016), highlights the importance of GI as a topic for investigation. Despite having multifunctional benefits, green areas are losing their importance in rapidly urbanized areas (e.g., megacities, metropolitan regions), and many GI areas (e.g., regeneration sites, vacant lots) are being transformed into GY areas due to the tangible economic benefits of such transformations. Therefore, it is vital to better understand how the scarcity of land for GI development and synergies among environmental, economic, and social services influence urban development agendas and help city leaders determine which development approach (GI or GY) might be most effective when transforming vacant lots and derelict sites (DS) (Meerow and Newell, 2017; Bardos et al., 2016).

Several studies have explored the suitability of developing and regenerating DS and vacant lots using multi-criteria evaluation (MCE) approaches to evaluate the potential of GI development in these sites (Anderson and Minor, 2017; Abebe, and Megento, 2017; Sanches and Pellegrino, 2016). These researchers have used weighted linear combination (WLC) and analytical hierarchy approaches (AHP) to define the importance and weight of various criteria to determine suitability (Beames et al., 2018; Kirnbauer and Baetz, 2014). However, selective weights are often based on an expert or analyst's subjective choice, social valuation (Langemeyer et al., 2016) and these approaches are vulnerable to potential biases. Furthermore, multi-criteria suitability approaches (WLC, AHP) do not allow researchers to understand trends and spatial changes over time; instead, they are used to recommend where GI or GY development should take place based on different types of potential benefits on a cross-sectional basis (Sanches and Pellegrino, 2016). Subjective judgment and lack of consideration for temporal change can produce biased results, meaning these methods may not be suitable for wider generalization when making future decisions regarding GI or GY development. In addition to multi-criteria based modelling approaches, simulation models such as cellular automate (CA), Agent Based Model and Genetic Algorithm are frequently used for simulating overall urban growth and understating patterns of multiple agents and cells, with multi-objective optimizations (Olmedo et al., 2015; Filatova et al., 2013; Mitsova et al., 2011; Cao et al., 2011; Vahidnia et al., 2013; Tseng et al., 2008). In particular Mitsova et al., (2011) demonstrated the use of CA in modelling urban growth and open space conservation, and they modelled the future scenarios based on GI conservation and no-conservation conditions. While these largescale simulation modelling are more frequent in understanding the city or regional land use change. However, these simulation approaches mostly are conducted at larger spatial scale and due to possible presence scale effects (e.g. considering larger cell sizes or larger patches of GI) these approaches are likely to be vulnerable to understand and predict single parcels of land within specific areas of the city (e.g. Derelict sites) (Mitsova et al., 2011; Dark and Bram, 2007). By contrast to WLC, AHP related Boolean logic-based methods and city/region wide urban land use change simulation modelling, we were focused on exploring the underlying trends and patterns of GI and GY development for individual sites within study area using multi-criteria, soft computing machine-learning approaches such as artificial neural networking (ANN) and Adaptive neuro-fuzzy modelling (e.g. ANFIS). These methods evaluate and identified the spatial trend of GI and GY development (e.g. in terms of land use change) for each individual sites/land parcels along waterways and derelict sites within the temporal frame of ten years (between 2007-2017) and evaluate these changes on the basis of crucial co-located factors or variables, such as surrounding tree coverage, accessibility, and population density. Then using the identified trend of land use change for every parcels along waterways and derelict sites and their co-located variables, the models were trained and later on the trained models predicted the possible future conditions of currently available vacant lands along the water ways and derelict sites. The potential key advantage of soft-computing models over WLC, AHP or CA that, these methods are entirely dependent on data-driven processes, where the weights of factors/criteria are determined from the trend observed in real world condition, rather than subjective choices of weights, and characteristics of forming transition rules (Mitsova et al., 2011) thus these data driven methods improve the robustness of the results in terms of not only identifying parcel based land use changes for GI or GY, but also clearly can predict potential future scenarios for sites that are still vacant or derelict (Melin et al., 2015; Jang et al., 1997).

Considering these, the aim of this research was to combine soft-computing machine learning methods (e.g., ANN) and multi-criteria GIS modelling to identify and model the trend of GI or GY development along linear waterways and DS and assess the likelihood of GI enhancement on the existing vacant or underdeveloped parcels along the waterways and derelict sites. As a case study, these methods were applied in the context of Manchester, England. This allowed the researcher to investigate previous and existing examples of GI and GY development in Manchester between 2007-2017 to identify sites that are more likely to be GI or GY, based on their co-located factors. Later on this allowed to improve the understanding about the vacant or derelict sites are more vulnerable to GY development, compared to improving GI quality of quantity. The findings may help Manchester City Council's (MCC) planning team make informed decisions regarding their GI action and implementation plans at specific sites or areas of the city, as well as set an example for other researchers focused on urban studies interested in implementing such a method. To our best knowledge, no such methodological process has been applied in GI-related studies.

2. GI Typologies, Values, and Determinants of development

In this research, GI type was determined based on Natural England's typologies. The primary GI typologies included parks and gardens, amenity spaces, natural and semi-natural urban green spaces, and green corridors (Mell, 2016). Different GI typologies have varying values and overlapping multifunctionality at different scales. Parks, urban gardens, and green corridors are found to provide greater multifunctionality in terms of ecological and social functions. Additionally, general amenity spaces and street trees are more valued at the micro/site scale. In contrast, DS and vacant lots provide the least ecological and economic benefits (Sanches and Pellegrino, 2016; Madureira and Andresen, 2014). Improving the least functional GI has become a major global initiative due to the potential for these spaces to enhance the overall quantity and quality of GI.

Usually, multiple determinates/variables influence GI development and planning, and these factors can be broadly categorised into five domains: ecological, environmental, social, economic, policy, and partnership (Quintas, 2015; Benedict and McMahon, 2012). Ecological determinants include site size, surrounding GI distribution (canopy coverage), and connectivity with other GI (Sanches and Pellegrino, 2016). Environmental factors motivating GI development include the need to improve microclimates, remove air pollution, and manage floodwater (Sinnett et al., 2015; Gill et al., 2007). From a social and community perspective, population density, overall accessibility (road coverage), surrounding land-use (built-up density), GI deprivation, health benefits, and protection of cultural values are important considerations for GI development (Quintas, 2015). Economic determinants are driven by issues such as ownership, property value improvement, proximity to city centres or high-value residential areas, and improvement costs (Longo and Campbell, 2017). Finally, policy and partnership determinants of GI are related to political ideologies, stakeholder relationships, and coordination among authorities (Mell, 2016). A summary of the relevant determinants for each domain is listed in Supplementary Table 1S.

3. Methods and Materials

3.1 Study Area

The study was conducted within the jurisdiction of Manchester City Council (MCC), which is at the core of the Greater Manchester city region. Manchester has a population of approximately 500,000, and it is one of fastest growing cities in the UK. Geographically, this core area is surrounded by city regions such as Salford, Stockport, and Trafford (Supplementary Figure 1Sa). Currently, 58% of the cityscape consists of GI (blue and green spaces, primarily tree canopy cover) with a river and canal network (Supplementary Figure 1Sb), highlighting the potential for an integrated GI network (MCC, 2017). Manchester also has large DS areas and undeveloped vacant lots along waterways (Raco et al., 2007), which require improvement to enhance overall GI quality and quantity and to benefit the environment. The MCC has repurposed DS and vacant lots using both Green (e.g., woodland) and Grey (e.g., commercial) approaches (Polyakova, 2011). However, GY development is more predominant. To address the imbalance, the MCC has formulated a GI development strategy for 2015-2025 focused on creating and enhancing a GI network (MCC, 2017).

3.2 Existing Waterway GI Network and Hub Identification

In order to explore the trend in GI development and predict future GI or GY development in relation to DS and vacant plots along WWCs, it was necessary to understand the existing condition of Manchester's GI network. Thus, an analysis of the GI patches, hubs, and corridors was conducted, and further definition of patch-corridor matrix is provided in *Supplementary Note 1*. These analyses identified the existing GI hubs and waterway corridors (WWCs) in Manchester. Multifunctional GI Hub (MGH) is a term coined in this research to define hubs that are similar to GI core/hubs (e.g., larger forest areas) in a GI network (Benedict and McMahon, 2012). However, MGH differs in terms of the spatial arrangement and proximity of different GI typologies. An

MGH is a hub that depends on the spatial density of various GI types, concentrated in particular areas. Burgess (2015), and Li et al. (2016) argued that GI hubs provide multifunctional benefits as they are agglomerations of several GI patches with greater densities of different GI elements. In this research, the kernel density estimation (KDE) function was used to estimate the density of existing GI elements in the study area. This function was computed using KDE in ArcGIS, a technique applied by several researchers modelling GI hubs and ecological density in conservation areas (Li et al., 2016; and Denoël and Ficetola, 2015). In this case, publicly accessible GI elements (i.e., parks, woodland, grassland, allotments, and outdoor sports areas) were considered. GI elements such as private gardens, green-roofs, amenity spaces, and institutional spaces were not included due to their restricted access and relatively lower contribution to the wider GI network. After KDE was calculated, the resulting density surface was divided into several classes using natural breaks, and higher density (Li et al., 2016) areas were identified as MGH.

In order to identify waterway corridors (WCCs), spline with barriers technique applied. This interpolation technique models GI networks (e.g., corridors), where the pixels represent values of certain GI elements, based on existing GI types provided as input. This pixel-based analysis method applied in the present study was similar to the morphological spatial pattern analysis utilized by Vogt et al. (2007), where bridges/corridors were identified as linked pixels that connect MGH. As GI elements often provide multifunctional benefits within a landscape matrix even if they are not directly connected, hence application of raster/pixel based interpolation conducted in the basis of the spatial continuity of the objects using vector objects (e.g., polygons) and interactivity of multifunctional benefits (e.g. Biodiversity connectivity, air purifications) in landscape matrix even if they are not directly (e.g. functionally) connected. The GI elements under consideration were recoded with numbers when transformed into points from polygons: Woodland: 5, Public parks and gardens: 4, Outdoor sports and playgrounds: 3, Allotments : 2, and Grassland : 1. These values indicated the importance of GI elements from the highest value to the lowest while taking into account the multifunctional benefits of each GI element. These numeric values were then interpolated using a spline with barrier function in ArcGIS. Barriers included any buildings or structures within the study area. Values in the interpolated surface represented various GI types and spatial connections among the pixels. From the connected pixels, corridors/bridges were identified (Vogt et al., 2007). The spline surface was divided into 10 classes for further conversion into polygons then allowing for spatial aggregation in ArcGIS. Pre-existing waterways formed connections between hubs (Such as rivers connecting multiple parks or institutional grounds), were included in the corridors. A buffer of 150 metres was delineated on each side of the corridor lines creating an overall corridor width of 300 meters, that was to be considered for WWCs need further enhancement.

3.3 Potential GI Intervention Sites Identification

Relatively lower functional and underdeveloped GI (e.g., general amenity spaces, grassland) which had centroids within the buffer zones of WWCs were, as part of the corridor, identified as sites for further enhancement. This was crucial to avoid selection of large GI polygon elements and to retain the original polygon geometry. In addition, 275 DS (Year 2013) were listed in the GI database by MCC at the time of the present study. However, it must be noted that several of them have already been utilized for GY development, and some of them are in the process of becoming GY. Therefore, not all 275 sites identified in 2013 are available for further enhancement. DS, defined as sites with buildings on less than 25% of their total area were identified to consider for enhancement. In this case, sites with only 25% built-up area versus 75% vacant space were considered by the present study to hold potential for future GI interventions.

3.4 Training and test (TT) sites selection

TT sites were sites selected to act as examples. Based on the values of the input variables the TT sites generated, intelligent systems would identify patterns and learn, allowing the intelligent systems to generate models that could provide simulations for sites with similar input variables. For WWCs, two categories of sites were selected (GI and GY). The polygon geometry of the GI elements with high multifunctionality (e.g., park and woodland in MCC 2013 database) were coded as one (1), and GY (e.g., buildings) represented by centroids within the buffer corridor were coded as zero (0). For derelict areas, TT sites were categorised as Derelict-to-Green (1) or Derelict-to-Grey (0). Several derelict areas marked by Gill et al. (2007) were transformed into GI or GY elements for the year 2013 (Updated GI database of MCC), thus providing examples of DS transformation.

3.5 Selecting Variables, Data Extraction, and Normalization

A literature review revealed that wide ranges of determinants/variables are associated with GI or GY interventions (Section 2). The variables used to develop and calibrate the present study's models and simulate future interventions were drawn from the literature presented in *Table 1A, Appendix A*. The selection of these variables was considered critical in light of existing literature. Site-size and canopy coverage are widely used ecological variables for the evaluation of GI elements (Benedict and McMahon, 2012). Air pollution levels are often considered critical and are consistently measured over long periods of time (Skelhorn et al., 2014). Population density, accessibility, and surrounding built-up conditions are variables found repeatedly in studies evaluating GI potential (Sanches and Pellegrino, 2016; Sinnett et al., 2015). Furthermore, a majority of the variables have spatial attribution. Such variables are of particular note for the present study as in this research, spatially explicit variables were considered particularly important.

For all TT and future intervention sites, the data values of the selected variables were extracted and normalized before modelling. TT and intervention site sizes were computed in ArcGIS. Canopy polygons were converted to point values and then into canopy density values utilizing a kernel density function and the *Canopy Area* as the population field. NO_2 concentration data was converted to One km^2 grid centroid raster values and then resampled to 20m raster. Population density was computed from ONS data to corresponding polygons, and then these polygons were transformed into a grid file. Accessibility was assumed to be representative of road density, proxy measurement for accessibility (Wang et al., 2016). In this case using line density functions, all roads in the study area are utilized to generate a raster surface to show road density. Finally, buildings around each site are again measured in terms of density, and kernel density has been utilized to generate building density raster. A buffer of 300 meters was considered to extract the values of each variable from the raster file for each site (TTs and potential sites) using the zonal statics tool in QGIS. After extracting data for each variable in GIS, the data were exported to Excel for further processing. Approaches such as ANN, ANFIS, and LR are often affected by overfitting if the data are not properly normalized. Therefore, the normalization of input data was essential prior to calibrating the model. In this case, a min-max normalization process was conducted on the entire dataset (Mohammady, 2016).

3.6 Modelling the likelihood of sites transformed to GI or GY

Based on the TT dataset, the ANN, ANFIS, and LR models were calibrated to simulate/estimate the future likelihood of potential intervention sites becoming GI or GY. The overall process used datasets from previous sections, then used SPSS (v23), MATLAB (R2017a), and ArcGIS (v10.2) and QGIS to model and plot the results in maps. The process is detailed in Figure 1.

[Figure 1 Near Here]

3.6.1 ANN Specifications

ANN is a data-driven, massive parallelism, machine-learning process that mimics biological neurons. Multilayer perceptron (MLP) is the most widely-used ANN method (Lee et al., 2014). MLP is used with supervised learning methods, with known input and outputs, and during the training of the network, node weights are adjusted based on error correction learning. MLP typically has three layers: input, hidden, output. The detail process of ANN is not covered in this paper; however, the technical details can be found in LeCun et al., (2015), Kechman, (2001) and *Supplementary Note 2*.

In this study two ANN models were developed, one for DS and one for WWC. The normalized TT data were randomly split into training (70%) and test (30%) sets using the partitioning function in SPSS (Figure 1b). The specific split between GI and GY was not considered in this case to maintain the simplicity of the models. Both models followed the same structure (Supplementary Figure 2S) with biases at input and hidden layers, a commonly used structure for MLP modelling. There is no exact rule to guide how many hidden layers should be in MLP. In this research, the researcher utilized one hidden layer, which is generally accepted for ANN, except for deep learning (LeCun et al., 2015). Activation functions were selected after experimentation, with tanH being selected for hidden layers and Softmax being selected for output layers. A gradient descent-based back propagation learning algorithm was utilized to train the model (Lee et al., 2014). After the models were trained and evaluated and minimum error against the test data was achieved, trained models were used to predict GI/GY intervention sites (Figure 1). Then, the estimated probability values for intervention sites (Likelihood of GI or GY) were imported into ArcGIS for mapping, with corresponding object ID numbers.

3.6.2 ANFIS Specifications

The neuro-fuzzy system incorporates fuzzy *membership functions* (MF) for given inputs and outputs, through the process of neural networking. ANFIS uses Tagaki and Sugeno-type fuzzy rules (Supplementary Figure 3Sa) that explain the conditions and consequences of mathematical functions in simple If-Then rules for different positions in membership function (Pradhan, 2013). Therefore, ANFIS can develop and optimize fuzzy rules that are easily interpretable in linguistic terms. This combines the benefits of neural networking and fuzzy logic, yielding greater explanatory power and robustness in reasoning (Jang, 1993; Jang, 1997).

ANFIS has five layers (Supplementary Figure 3Sb). Layer-1 takes the crisp input values (e.g., Canopy density) and converts them into fuzzy MF (*A1, A2*) (e.g., Gaussian, triangle). In Layer-2, If-Then rules are employed, and initial weight/firing strengths (*w1, w* 2) are computed based on input from Layer-1. Layer-3 normalizes the weight to make it consistent among different MF. In Layer-4, defuzzification takes place, and If-Then rules are adjusted for output layers. Finally, Layer-5 shows defuzzified linear output values, where the output is the sum of all products of normalized weights and fuzzy rules (Details in Jang, 1997).

In this study, normalized TT dataset for DS and WWC sites were randomly split into training (more than 70%), test, and validation datasets (Figure 1c). Using the training dataset for DS and WWC sites, Sugeno-type Fuzzy Interface System (FIS) structures were generated for two ANFIS models in MATLAB. The development of FIS was conducted based on a subtractive clustering (SC) method (Chiu, 1994). SC works better with independent variables greater or equal to six (Vaidheihi, 2014; Jang, 1995). Additionally, SC methods automatically generate membership functions (MF), allowing the dataset to decide how many MFs are required for training. Three input MF (inputmf) were generated for *ANFIS1* for WWC, and two inputmf were generated for *ANFIS2* for DS for input Layer-1. For both models, Gaussian MF was utilized for input and output MFs, as recommend by Jang (1993), because it provides better results with the hybrid learning algorithm used for these models. The outputs of these models were linear. The models were set to run for 100 epochs (iterations) and to achieve a minimum RMSE value that was as close to zero as possible. The overall MATLAB codes for the FIS file of ANFIS1 and ANFIS2 are provided in Supplementary Code Box1 and Box2 respectively.

After the models were trained, using input values of derelict potential intervention sites, ANFIS2 simulated/predicted the likelihood of transformation to GI or GY, and ANFIS1 used input values of potential intervention sites along WWCs to simulate their likelihood to transform into GI or GY. Later, these simulated/predicted output values were normalized exported in ArcGIS for mapping.

3.6.3 Logistic Regression (LR) specifications

In order to compare machine learning methods with traditional statistical models, LR was utilized. LR is a computationally different method than ANN and ANFIS. LR is a probabilistic method that estimates and demonstrates relationships between independent and dependent variables. Unlike linear regression, LR can handle nonlinear data sets. LR is a widely used method in land use modelling and image classification (Mohammady, 2016). LR can also complement ANN and ANFIS results, demonstrating the effectiveness of traditional statistical models when forecasting for short periods (Arsanjani et al., 2013).

Two binary LR models were developed to explore the relations among independent and dependent variables (Figure 1d), as well as to predict GI and GY probability, using the probability function (Eq 1) (Lee, 2005).

$$P = exp\frac{(B_0+\sum_{i=1}^{n} B_i X_i)}{1+exp(B_0+\sum_{i=1}^{n} B_i X_i)} \dots \dots (Eq1)$$

Where, ***P*** is the probability of a particular change (i.e., GI or GY), Xi is the parameters of change (e.g., Canopy Density), B_0 is constant, and B_i is the coefficient of each parameter. ***P*** is estimated to be between 0 to 1 (Arsanjani et al., 2013; Lee, 2005). In SPSS, the model was calibrated for all TT sites. Then, using the values of the independent variables for the potential sites, probabilities were estimated and the resulting values were exported to GIS for mapping.

3.7 Validation of the Models

In order to validate the models, we considered three criteria. First, Root Mean Square Errors (RMSE) values were checked for all the models. The model with lowest RMSE values was considered the best-fitted model. Second, we considered similarity and dissimilarity among the model predictions for potential intervention sites. In this way, the relative performances of the models in terms of prediction were evaluated. Third, we applied McNemar's test of paired prediction to evaluate whether the model outputs actually differed (Rozenstein and Karnieli, 2011). Apart from these measures the overall classification accuracy of training and test data were checked for the ANN and LR models.

4. Results

4.1 GI Network and WWCs

A GI network map (from GI elements, Supplementary Figure 4Sa) indicating the *Multifunctional GI Hubs (MGHs)* and possible ecological corridors was produced according to KDE analysis. It was observed that MGHs usually provided multiple functions (e.g., recreation). Our results were consistent with Li et al. (2016) who argued that multiple functions of GI may be observed in areas with varying GI elements in close proximity. In total, 13 MGHs were found in the MCC area, and the connections among MGHs often followed waterways.

Taking barriers into consideration (Figure 2a), the spline interpolation results more clearly illustrated GI elements and their internal connections (Figure 2b). After coversine and aggregation of the spline grid, polygons showed existing WWCs and GI networks along waterways (Figure 2c). Considering GI along waterways, connected polygons, and a 300m buffer along corridor lines, the WWCs in MCC are illustrated in Figure 2d. One major pre-existing WWC was found along the Mirsey River that connects two major GI hubs. Additionally, the Medlock and Irk rivers, along with two canals, were main WWCs.

[Figure 2 Near Here]

4.2 Identified Potential Intervention Sites

We identified potential intervention sites along WWCs and among the DS in Manchester. Along the WWCs, interventions sites are currently low-value GI elements (e.g., pioneer grassland, vacant riparian site). Thus, the sites might possibly undergo further GI enhancements or GI transformation to obtain better GI functionality. In total, 150 WWCs sites were identified and considered for further intervention (Supplementary Figure 5S-a). For DS, 112 sites were identified that were either completely vacant (no structure) or consisted of more than 75% vacant space (Supplementary Figure 5S-b). DS were often scattered, but in some cases, several sites were closely grouped.

4.3 Training and Test Sites and Modelling Data Extraction

In this study, for TT sites, we obtained 3916 (1009 GI and 2907 GY) sites along WWCs and 866 DS (442 GI, 424 GY) (Supplementary Figure 6S). Attributes or values for these sites were extracted based on the selected modelling input variables in order to train and test the models for future predictions.

Site sizes were directly computed without mapping; and it has been observed that, majority of WWC sites being GI are greater in size compared to GY sites. However, for DS such difference is not prominent between GI and GY. Canopy density is presented in Figure 3a. Higher densities were observed close to WWCs and Manchester's middle zone, which consisted mostly of residential areas, Comparing with UMT, Gill et al., (2007). Figure 3b shows NO_2 concentration. Most areas had low NO_2 concentration, except city centres. Areas near waterways had the lowest NO_2 concentration. Figure 3c illustrates that population densities were highest around residential areas and lowest near MGHs and city centre areas. Road and building densities were found to be very high near city centre zones, and lowest along WWCs (Figure 3d,e). These densities were similar in their spatial pattern; higher building density was followed by higher road density, and vice-versa.

[Figure 3 Near Here]

4.5 Model Results for Patter understanding and Prediction

We calibrated three sets of models ANN, ANFIS and LR to train, test, and predict the future conditions of GI or GY for WWCs and DS. The calibrated ANN models used training and test datasets to produce trained neural networks that predicted the GI/GY likelihood values (probability) for potential sites. The ANN models for WWCs resulted in 89.3% accuracy for training and 89% accuracy for testing (Supplementary Table 2S). Similar to WWC, the ANN model for DS using the trained neural network obtained 90.3% accuracy in training and 91.8% accuracy in testing (Supplementary Table 2S). Both of these models predicted values for the intervention sites based on the pattern of existing GI or GY development along WWCs and DS. The predicted values were then exported to AcrGIS for mapping. Predicted values for potential sites along WWCs and DS are illustrated in Figure 4c,d. Out of five probability categories, the ANN models predicted that 62% (n = 93 of 150) of intervention sites along WWCs have a very high likelihood of transforming into GI. In contrast, 34.8% (n = 39 of 112) of DS have a very high likelihood of becoming GI (Supplementary Table 4S).

Using the normalized training and test data, we calibrated ANFIS models for WWCs and DS. In both cases, ANFIS models were expected to require hundreds of epochs during training. For the WWC training data, between epochs 18-20, were needed to reduce the error to a minimum (RMSE 0.29, ANFIS1), after which point it remained consistent for the remaining iterations (Supplementary Figure 7S-a). The DS training and test data were also calibrated using 100 epochs, and for this model, the minimum RMSE was reached between epoch 72 and 75. Error started at about 0.4 and was reduced to 0.28 after training (ANFIS2, Supplementary Figure 7S-b). For ANFIS1, the minimum error for the prediction was 0.29, while for ANFIS2, the minimum error during prediction was 0.28. Validation datasets for both models were utilized during the training process (15% of all data), to observe and control overfitting of the ANFIS models.

Both the ANFIS1 and ANFIS2 models tuned and optimized all fuzzy membership functions to fit the relationships between the dependent and independent variables during the training process. By doing so, the models found membership functions that were a close fit to the output. The resulting fuzzy rules of input layers contribute to form the values of output rules and estimate outputs. Two examples are provided in Supplementary Figure 8S. Once the calibration of both models was conducted, using these rules, GI/GY likelihoods for the potential interventions sites were simulated in MATLAB. These predicted values were then extracted and mapped in ArcGIS (Figure 4a,b) as map formats for spatial relation exploration. Comparisons between the probability classes for intervention sites showed that for WWCs, 28.7% of sites (n = 43 of 150) had a very high likelihood of becoming GI and 40.7% of sites (n = 61 of 150) had a high likelihood of becoming GI. In contrast, 32.1% of DS sites (n = 36 of 112) had a very high likelihood of becoming GI, and only 20.5% of sites (n = 23 of 112) had a high likelihood of transforming into GI (Supplementary Table 4S). Both of these modelling approaches predicted a higher probability that WWCs sites would become highly functional GI in the near future, while the DS had a greater likelihood of becoming

GY. However, there were clear differences in the outputs between ANN and ANFIS. These differences are discussed further in the model evaluation section.

[Figure 4 Near Here]

Our calibrated LR summaries are presented in Table 1. For WWCs sites, all variables except canopy density and road density were statistically significant ($p < 0.05$), and site size and air pollution level positively contributed to sites becoming GI. Conversely, building density and population density negatively affected a site's likelihood of becoming GI along WWCs (Reference category is GY). This explains that for WWC sites, larger site size, higher air-pollution, lower building density, and lower population density increase the likelihood of a site becoming GI. Overall, for WWCs, LR accurately classified 81.9% of sites and explained 31% of the variance [Pseudo R-Square] in GI/GY transformation. Classification accuracy for GI was significantly less (37.6%, Supplementary Table 3S). Therefore, it was concluded that the LR model predicted GI poorly.

[Table 1 Near Here]

Similarly, for DS, LR was calibrated using TT data to predict the probabilities of potential sites. Table 1 shows all the variables were statistically significant (p <0.05) for DS, based on the Wald test. Building density and road density negatively affected the possibility of being GI, compared to GY. Site size, canopy density, population density, and higher air pollution positively influenced the possibility of being GI (*B*, Table 1). The odd ratio shows that the effect of site size is much too high compared to any other variable in the model, indicating site size is the main predictor for GI and GY. The LR model classified 82.6% (Supplementary Table 3S) of DS accurately and can explain 54.6% of the variance of GI/GY transformation. Using the calibrated LR models for both cases, predictions for intervention sites along WWCs and DS were estimated and then exported to be mapped in ArcGIS (Figure 5). In this case, the differences were even greater. In total, 58.7% (n = 88 of 150) of WWCs had a likelihood of transforming in to GI, whereas only 19.6% (n = 22 of 112) of DS had a likelihood of becoming GI (Supplementary Table 4S).

[Figure 5 Near Here]

4.6 Evaluation of the Models

The evaluation of the models clearly showed the differences among modelling techniques when making predictions for the intervention sites. For evaluation, we used a cut value of 0.5 to obtain clear classification between GI and GY for the intervention sites based on the estimated values of different models. The RMSE values showed that for WWCs, ANN performed better than other models in terms of RMSE. However, ANFIS1 had very similar RMSE values compared to ANN and showed greater similarity (nearly 90%) to other models. The McNemar's test of paired prediction showed that in this case, the ANN and ANFIS1 were not significantly different from each other, but significant difference (p <0.1) was found between LR and ANN and ANFIS1 (Table 2). In case of DS, again ANN had the lowest RMSE values. In contrast to the WWCs models, for DS, ANN also had the highest similarity among the models. The McNemar's test showed significant differences between ANN and ANFIS ($p < 0.1$), and there were clearly very strong differences between the ANN, ANFIS2, and LR models ($p < 0.001$; Table 2). LR produced higher RMSE values and exhibited major differences when predicting GI or GY transformation for DS. Comparing all the models, it can be argued that in both cases, the ANN models had the lowest errors in the prediction and training processes. However, the ANFIS models produced similar results but were more robust in terms of explaining the reasons behind results. Furthermore, the membership functions in ANFIS allowed us to show the differences, while the ANN models are totally black box. In both cases, the traditional statistical method of LR performed poorly, indicating its inability to learn the pattern and predict actual phenomenon in the datasets. Thus, data-driven models are more robust and suitable for such conditions.

[Table 2 Near Here]

5. Discussions and Policy Implications

5.1 Potential GI interventions and Critical GI/GY predictors

WWC sites (N = 150) had higher GI transformation likelihoods compared to DS (N = 112) in all three models. Conversely, GY transformation likelihoods were higher for DS than for WWC sites (Table 2A, Appendix). Using these results, the MCC can decide whether to enhance WWCs as part of an integrated GI network development or to protect and enhance DS, which are more likely to transition to GY due to their location. This can further develop their GI policy refinement and enhancements. Findings from this study mirror the observed reality in Manchester, where many

DS are now undergoing major construction (confirmed by field visits to some of the development sites in 2017).

The ANFIS and LR models indicated the relative importance of the independent variables/criteria used in this study. For site size, fuzzy membership functions were mostly optimized, resulting in a very large odd ratio, indicating site size is the main variable of a site becoming GI/GY. Anderson and Minor (2017) and Benedict and McMahon (2012) also illustrated such observations for GI development. Air pollution and population density were found to be the next most important (moderate optimization in ANFIS) while building density, canopy density, and road density had the lowest importance among all the models. The importance of air pollution and population density has previously been observed when selecting GI interventions for air purification (Pugh et al., 2012). However, we acknowledge that often the reverse is possible; as GI areas often purify air pollution, they can be co-located. We also observed that to serve a greater number of people, GI investment decisions are usually made in densely populated areas on small vacant sites, which is the case for DS (Anderson and Minor, 2017). In our case, similar predictions for DS intervention were been made by ANN and ANFIS models. We also observed contrasting findings for WWCs in such cases. As WWCs and population are negatively related variables, the spatial pattern shows that WWC intervention sites are often far away from residential zones and not promoted for residential development. Lower population density is observed around these sites.

Building density negatively influenced GI investment decisions, indicating GI development is more likely to occur in open areas in contrast to more densely built areas. This has also been found in Sinnett et al., (2015). The results indicated that landscape location does affect GI/GY transformation, as sites near dense urban areas (e.g., city centers) were more likely to be GY due to their economic benefits and land price (Longo and Campbell, 2017). While road density and accessibility have been emphasized as important for GI interventions in study by Cetin (2015), we found accessibility for distant locations along WWCs was not well established, and often these sites were less accessible for people. Therefore, the models did not recognize road density as an important predictor. For DS, which are already located near well-developed road networks, accessibility was important and did promote more grey development initiatives.

5.2 Model Strengths and limitations

Utilizing robust models such as ANN and ANFIS, which are less capable of explaining causes of GI/GY transformations but more predictive regarding trends/pattern, can help formulate better policies, improve landscape planning, and guide future investment decisions. Considering the many advantages of these models over traditional statistical methods that are prone to inaccuracy (e.g., Linear Regression and LR) or more complex methods that require a greater number of assumptions and data (e.g., Agent Based Model) (Harrell, 2015; Bonabeau, 2002). It can be argued that ANN and ANFIS deserve more attention when conducting empirical studies in the areas of GISc.

This study is more predictive in nature and less explanatory, and we encountered several limitations. The reasons behind the ANN outcomes were not well explained in terms of causation due to the model's black box nature. Furthermore, machine learning models were trained using randomly drawn rows, and with different randomization, the classifications and error values had slight variations and less generalization capacity (Donate et al., 2013). In addition, unequal sampling between WWC and DS training and test sites produced vulnerability of the ANN and ANFIS models to show a classic symptom of machine learning models to better recognize the majority class. Furthermore, only six criteria/predictors were considered due to time limitations. Relatively low numbers of TT sites (considering vast data requirement of machine learning algorithms) were considered because of data unavailability and selective study site. We recognize these limitations and indicate improvements for future studies, such as conducting K-fold cross-validation for training and testing datasets and examining the effect of different training sets on model accuracy and generalized modelling errors. It is also recommended that more criteria (e.g., land price) and more observations be added to the modelling process to improve the predictive and explanatory power of models.

6. Conclusion

This study utilized and evaluated soft-computing, machine-learning methods integrated with spatial analytical tools to understand the current policy trend in GI/GY development, and explore GI enhancement possibilities along WWCs and DS in Manchester. Analysing spatial data and modelling the likelihood of GI at different study sites, we found that the multicriteria-based machine learning models ANN and ANFIS work better for understating the spatial patterns of GI and GY development. Site size, population density, and air pollution were the main predictors of GI/GY transformation in this study's context. Our study also implied that future intervention sites along WWCs in Manchester have a higher likelihood of transforming into GI, whereas DS are more likely to become GY. This indicates that the patterns learned by the models are representative of current planning decisions in Manchester, with DS being transformed into high-value GY to generate economic benefits. The MCC's current planning policies might ignore DS improvements in favour of higher-value GI elements such as pocket parks that can more easily be connected to the existing GI network. Ultimately, the vacant and less improved large sites along waterways have received less attention from the MCC, despite the potential for multifunctional benefits that could be created when integrating blue-green networks in Manchester to have better ecology, biodiversity, and social benefits. This study can be replicated globally to add new understanding to the future of GI trends and urban environmental sustainability for generations to come.

References

Abebe, M.T. and Megento, T.L., 2017. Urban green space development using GIS-based multi-criteria analysis in Addis Ababa metropolis. *Applied Geomatics, 9*(4), pp.247-261.

Anderson, E.C. and Minor, E.S., (2017). Vacant lots: An underexplored resource for ecological and social benefits in cities. *Urban Forestry & Urban Greening, 21*, pp.146-152. DOI: https://doi.org/10.1016/j.ufug.2016.11.015

Bardos, R.P., Jones, S., Stephenson, I., Menger, P., Beumer, V., Neonato, F., Maring, L., Ferber, U., Track, T. and Wendler, K., (2016). Optimising value from the soft re-use of brownfield sites. *Science of The Total Environment, 563*, pp.769-782. DOI: https://doi.org/10.1016/j.scitotenv.2015.12.002

Beames, A., Broekx, S., Schneidewind, U., Landuyt, D., van der Meulen, M., Heijungs, R. and Seuntjens, P., (2018). Amenity proximity analysis for sustainable brownfield redevelopment planning. *Landscape and Urban Planning*, *171*, pp.68-79. DOI: https://doi.org/10.1016/j.landurbplan.2017.12.003

Benedict, M.A. and McMahon, E.T., (2012). *Green infrastructure: linking landscapes and communities*. Island Press.

Burgess, S., (2015). Multifunctional green infrastructure: a typology. *Handbook on Green Infrastructure: Planning, Design and Implementation*, p.227.

Cetin, M., (2015). Using GIS analysis to assess urban green space in terms of accessibility: case study in Kutahya. *International Journal of Sustainable Development & World Ecology, 22(5)*, pp.420-424. DOI: http://dx.doi.org/10.1080/13504509.2015.1061066

Chiu, S.L., (1994). Fuzzy model identification based on cluster estimation. *Journal of Intelligent & fuzzy systems, 2(3)*, pp.267-278. DOI: 10.3233/IFS-1994-2306

Denoël, M. and Ficetola, G.F., (2015). Using kernels and ecological niche modeling to delineate conservation areas in an endangered patch-breeding phenotype. *Ecological Applications, 25(7)*, pp.1922-1931. DOI: 10.1890/14-1041.1

Donate, J.P., Cortez, P., Sanchez, G.G. and De Miguel, A.S., (2013). Time series forecasting using a weighted cross-validation evolutionary artificial neural network ensemble. *Neurocomputing, 109*, pp.27-32. DOI: https://doi.org/10.1016/j.neucom.2012.02.053

Harrell, F., (2015). *Regression modeling strategies: with applications to linear models, logistic and ordinal regression, and survival analysis*. Springer.

Jang, J.S., (1993). ANFIS: adaptive-network-based fuzzy inference system. *IEEE transactions on systems, man, and cybernetics, 23(3)*, pp.665-685. DOI: 10.1109/21.256541

Jang, J.R., (1997). *MATLAB: Fuzzy logic toolbox user's guide: Version 1*. Math Works.

Jang, J.S. and Sun, C.T., (1995). Neuro-fuzzy modeling and control. *Proceedings of the IEEE, 83(3)*, pp.378-406. DOI: 10.1109/5.364486

Jang, J.R., Sun, C.T. and Mizutani, E., (1997). Neuro-fuzzy and soft computing: a computational approach to learning and machine intelligence.

Kirnbauer, M. and Baetz, B., (2014). Prototype decision-support system for designing and costing municipal green infrastructure. *Journal of Urban Planning and Development, 140(3)*, p.04014004. DOI: https://doi.org/10.1061/(ASCE)UP.1943-5444.0000191

LeCun, Y., Bengio, Y. and Hinton, G., (2015). Deep learning. *Nature, 521(7553*), pp.436-444. DOI:10.1038/nature14539

Lee, S., (2005). Application of logistic regression model and its validation for landslide susceptibility mapping using GIS and remote sensing data. International Journal of *Remote Sensing, 26(7)*, pp.1477-1491. DOI: http://dx.doi.org/10.1080/01431160412331331012

Lee, S., An, H., Yu, S. and Oh, J.J., (2014). Creating an advanced backpropagation neural network toolbox within GIS software. *Environmental earth sciences, 72(8)*, pp.3111-3128. DOI: 10.1007/s12665-014-3216-7

Li, P., Lv, Y., Zhang, C., Yun, W., Yang, J. and Zhu, D., (2016). Analysis and Planning of Ecological Networks Based on Kernel Density Estimations for the Beijing-Tianjin-Hebei Region in Northern China. *Sustainability, 8(11)*, p.1094. DOI:10.3390/su8111094

Longo, A. and Campbell, D., (2017). The determinants of brownfields redevelopment in England. *Environmental and Resource Economics*, 67(2), pp.261-283. DOI: https://doi.org/10.1007/s10640-015-9985-y

Madureira, H. and Andresen, T., (2014). Planning for multifunctional urban green infrastructures: Promises and challenges. *Urban Design International, 19(1)*, pp.38-49.

MCC(Manchester City Council). (2017). Manchester's 'Green and Blue Infrastructure' strategy | 'Green and Blue Infrastructure' consultation | Manchester City Council. Available at: http://www.manchester.gov.uk/info/200024/consultations_and_surveys/6905/green_and_blue_infrastructure_consultation [Accessed 12 January 2018].

McDonald, R.I., Kareiva, P. and Forman, R.T., (2008). The implications of current and future urbanization for global protected areas and biodiversity conservation. *Biological conservation, 141(6)*, pp.1695-1703. DOI: https://doi.org/10.1016/j.biocon.2008.04.025

McKinney, M.L., (2002). Urbanization, biodiversity, and conservation: the impacts of urbanization on native species are poorly studied, but educating a highly urbanized human population about these impacts can greatly improve species conservation in all ecosystems. *Bioscience, 52(10)*, pp.883-890. DOI: https://doi.org/10.1641/0006-3568(2002)052[0883:UBAC]2.0.CO;2

Meerow, S. and Newell, J.P., (2017). Spatial planning for multifunctional green infrastructure: Growing resilience in Detroit. *Landscape and Urban Planning*, 159, pp.62-75. DOI: https://doi.org/10.1016/j.landurbplan.2016.10.005

Mell, I. C., (2016). *Global Green Infrastructure: Lessons for successful policy-making, investment and management*. Routledge.

Mohammady, S., (2016). Optimization of adaptive neuro fuzzy inference system based urban growth model. *City, Territory and Architecture*, 3(1), p.10. DOI: 10.1186/s40410-016-0039-8

Nielsen, A.B., Hedblom, M., Olafsson, A.S. and Wiström, B., (2017). Spatial configurations of urban forest in different landscape and socio-political contexts: identifying patterns for green infrastructure planning. *Urban Ecosystems, 20(2)*, pp.379-392. DOI: 10.1007/s11252-016-0600-y

Polyakova, A. (2011). *Assessing the Potential Climate Change Adaptation Functions of Green Spaces Redeveloped from Brownfields in Greater Manchester*. Unpublished M.Sc thesis, University of Manchester.

Pradhan, B., (2013). A comparative study on the predictive ability of the decision tree, support vector machine and neuro-fuzzy models in landslide susceptibility mapping using GIS. *Computers & Geosciences, 51*, pp.350-365. DOI: https://doi.org/10.1016/j.cageo.2012.08.023

Pugh, T.A., MacKenzie, A.R., Whyatt, J.D. and Hewitt, C.N., (2012). Effectiveness of green infrastructure for improvement of air quality in urban street canyons. *Environmental science & technology, 46(14)*, pp.7692-7699. DOI: 10.1021/es300826w

Quintas, A., (2015). Planning for urban green infrastructure in metropolitan landscapes. *Handbook on Green Infrastructure: Planning, Design and Implementation*, p.184.

Raco, M., Henderson, S. and Bowlby, S., (2007). Delivering brownfield regeneration: sustainable community-building in London and Manchester. Sustainable Brownfield Regeneration*: Liveable Places from Problem Spaces*, pp.119-139.

Sanches, P.M. and Pellegrino, P.R.M., (2016). Greening potential of derelict and vacant lands in urban areas. *Urban Forestry & Urban Greening*, 19, pp.128-139. DOI: https://doi.org/10.1016/j.ufug.2016.07.002

Sinnett, D., Smith, N. and Burgess, S. eds., (2015). *Handbook on Green Infrastructure: Planning, Design and Implementation*. Edward Elgar Publishing.

Skelhorn, C., Lindley, S. and Levermore, G., (2014). The impact of vegetation types on air and surface temperatures in a temperate city: A fine scale assessment in Manchester, UK. *Landscape and Urban Planning, 121*, pp.129-140. DOI: https://doi.org/10.1016/j.landurbplan.2013.09.012

Tzoulas, K., Korpela, K., Venn, S., Yli-Pelkonen, V., Kaźmierczak, A., Niemela, J. and James, P., (2007). Promoting ecosystem and human health in urban areas using Green Infrastructure: A literature review. *Landscape and urban planning*, 81(3), pp.167-178. DOI: https://doi.org/10.1016/j.landurbplan.2007.02.001

Vogt, P., Riitters, K.H., Estreguil, C., Kozak, J., Wade, T.G. and Wickham, J.D., (2007). Mapping spatial patterns with morphological image processing. *Landscape ecology, 22(2)*, pp.171-177. DOI: 10.1007/s10980-006-9013-2

Acknowledgements

The author like to express humble gratitude to Dr. Sarah Lindley, at the University of Manchester, for her patient, circumspective guidance, amiable support and affectionate encouragement in designing this study and writing the paper. In addition, heartiest thanks to Dr. Angela Harris for her insightful comments during the research work and correcting some of the aspects of the research. The author also like to acknowledge the data support of EDINA, Ordnance Survey, ONS, Defra. Specially GI data of Manchester City Council, details tree database from City of Trees, UTM dataset of Gill et al., (2007) and SEED-shared data without these data the study would not be possible to conduct. Finally, the author would also like to thank the three anonymous reviewers of this paper for their constructive comments and suggestions, their comments and suggestions helped improving the paper.

Figures

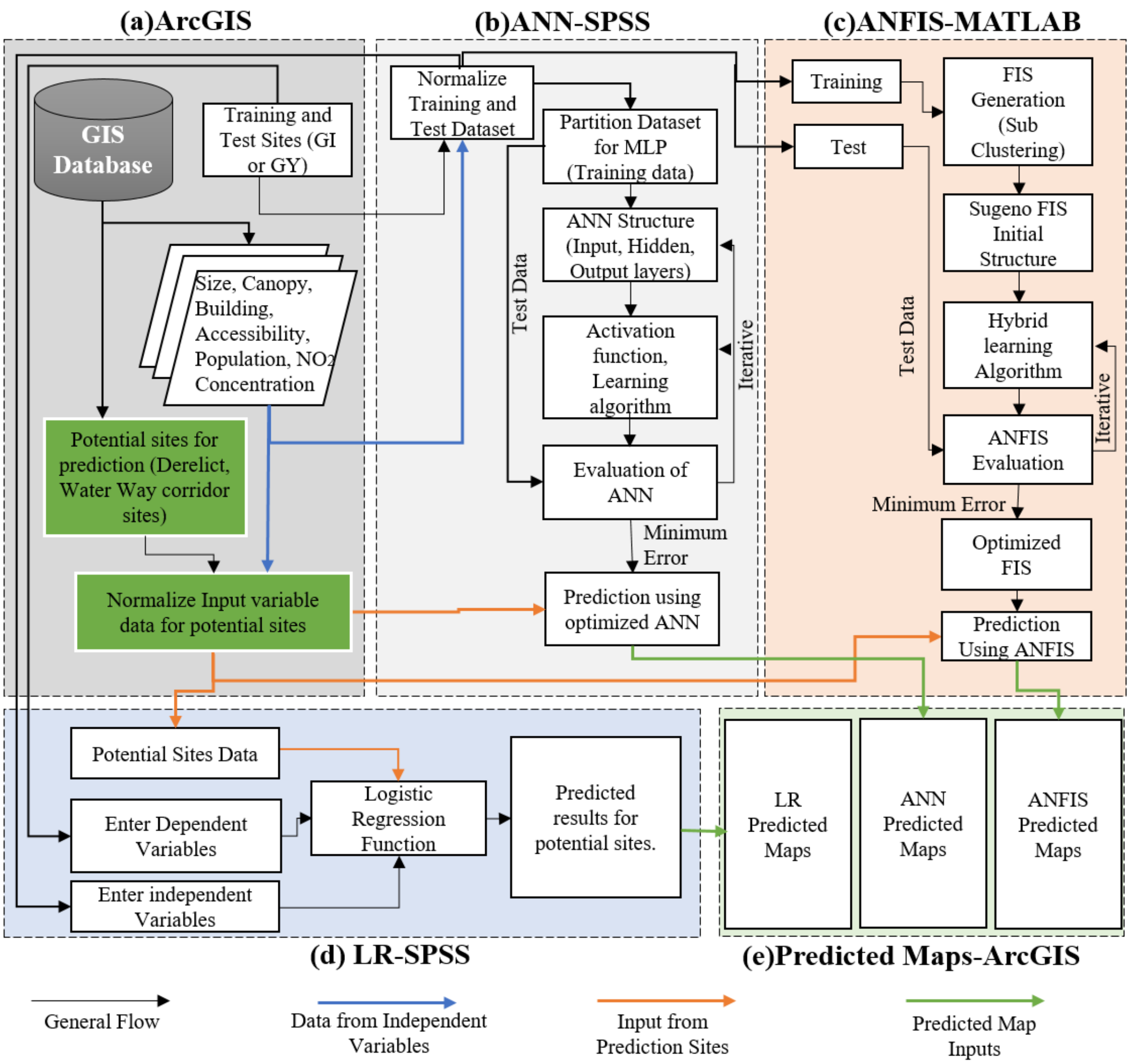

Figure 1: Flow diagram of data processing, integration, modelling and prediction. (a) GIS database of all TT, intervention sites, and determinants. (b) Normalized database, split in training and test data, to be developed ANN and the process of running ANN (c) ANFIS model calibration and prediction (d) logistic regression analysis process in SPSS, (e) Predicted maps for intervention sites using logistic regression, ANN and ANFIS generated in GIS.

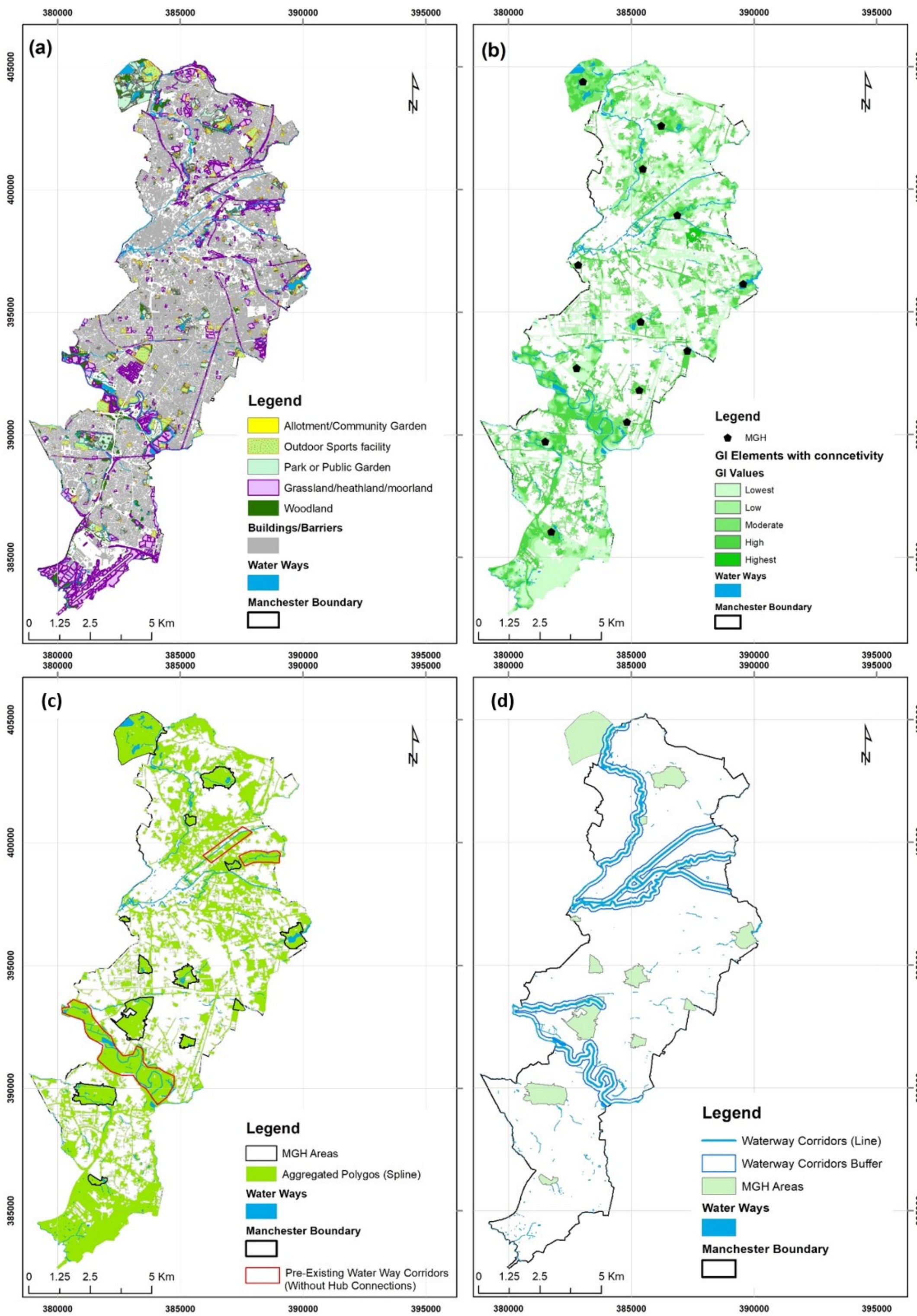

Figure 2: (a) GI elements with barriers (b) Spline interpolation results (c) Aggregated polygons from spline interpolation (d) Identified WWCs in MCC.

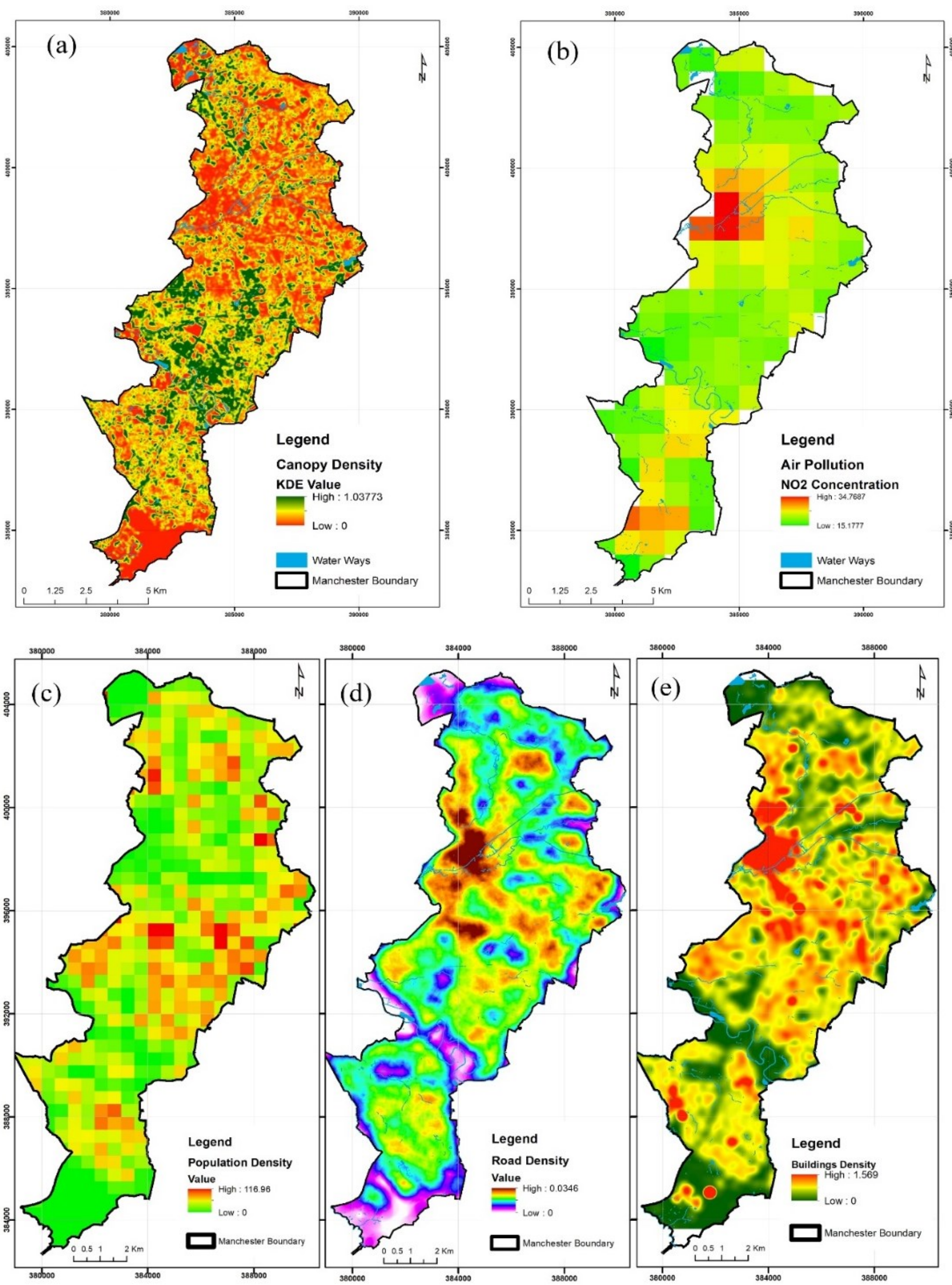

Figure 3: (a) Canopy density (per-km^2) in Manchester (b) NO_2 concertation ($\mu g\ m^{-3}$) in Manchester. (c) Population density (d) Road density (per-km^2) (e) Building density (per-km^2) in Manchester.

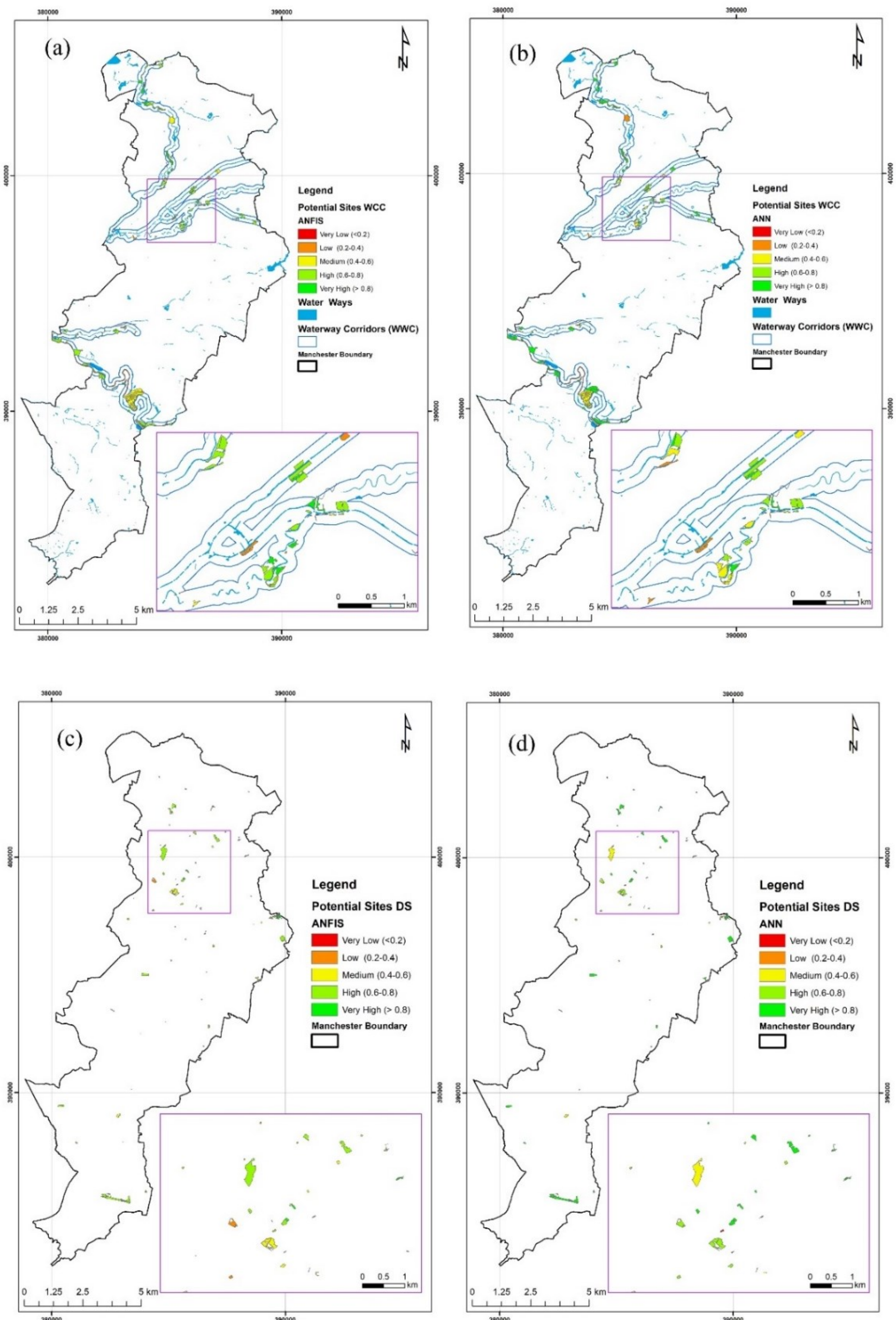

Figure 4: (a) The likelihood of WWC intervention sites becoming GI based on ANFIS. (b) The likelihood of WWC intervention sites becoming GI Based on ANN. (c) The likelihood of DS

intervention sites becoming GI based on ANFIS. (d) The likelihood of DS intervention sites becoming GI based on ANN.

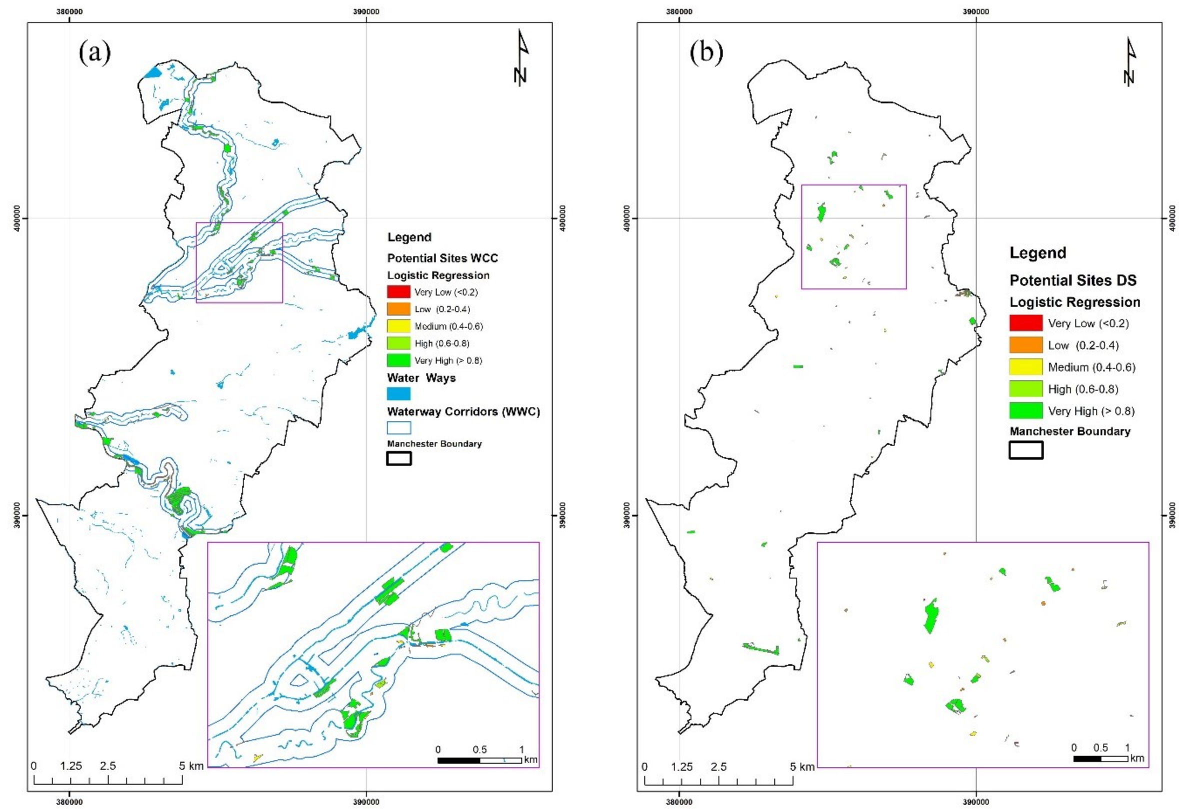

Figure 5: (a) The likelihood of WWCs intervention sites becoming GI according to LR model. (b) The likelihood of DS becoming GI according to LR.

Tables

Table 1: Logistic Regression results for WWCs and DS.

Variables	Waterway Corridors				Derelict Sites			
	B	**S.E.**	**p**	**Exp(B) [Odd Ratio]**	**B**	**S.E.**	**p**	**Exp(B) [Odd Ratio]**
Site Size (SS)	119.12	7.089	.000	$5.423*E^{51}$	88.774	8.782	0.000	$3.583*E^{38}$
Canopy Density (CD)	.460	.280	.100	1.584	1.473	.632	0.020	4.364
Building Density (BD)	-4.206	.340	.000	.015	-3.602	.927	0.000	.027
Road Density (RD)	.536	.514	.297	1.709	-5.483	1.023	0.000	.004
Population Density (PD)	-1.160	.265	.000	.314	2.942	.790	0.000	18.950
Air Pollution (AP)	1.091	.304	.000	2.976	3.606	1.398	0.010	36.831
Constant	-0.435	.210	.038	.647	-1.419	.996	.154	.242
Nagelkerke R^2	0.31				0.546			
n	3916				866			
B = Coefficient, S.E = Standard Error, df = Degree of Freedom								

Table 2: Evaluation of all models

	Model	RMSE	Similarity with other models			Statistical significance of difference		
			ANN	**ANFIS**	**LR**	**ANN**	**ANFIS**	**LR**
Waterway Corridors based models	**ANN**	0.285	-	-	-	-	-	-
	ANFIS1	0.29	90.66%	-		0.791	-	-
	LR	0.364	74.66%	89.33%	-	0.089*	0.077*	-
Derelict Site based models	**ANN**	0.235	-	-	-	-	-	-
	ANFIS2	0.285	80%	-	-	0.093*	-	-
	LR	0.350	74%	68%	-	0.000**	0.000**	

Appendix A

Table 1A. Selected Input variables considered in this study, their data type and sources.

Domain	Variables	Format	Year	Sources
Ecology	Site Size	ESRI(Polygons)	2015	MCC
	Surrounding Tree Coverage	Geo-database (Polygons)	2015	City of trees[1]
Environmental	Air pollution, ($N0_2$) concentration	CSV file	2016	Defra[2]
Social and Community	Population density (Census Data)	Excel File	2011	Office for National Statistics (ONS)
	Accessibility (in terms of Road Density)	ESRI(Polyline)	2011	Edina[3]
	Surrounding Built up area (Building density)	ESRI(Polygons)	2011	Edina

[1] Formerly Red Rose Forest, a community forest in western and central Greater Manchester,

[2] Department for Environment, Food and Rural Affairs,

[3] EDINA and Data Library is a center of digital expertise for UK Higher Education.

Table 2A: Comparing the likelihood of GI/GY transformations for potential sites

Site for Considerations	Type of transformations	ANN		ANFIS		LR	
		n	**%**	**n**	**%**	**n**	**%**
Potential sites along WWCs (Total 150 sites)	**GY**	29	19.3	31	20.7	39	26
	GI	121	80.7	119	79.3	111	74
Potential DS (Total 112 sites)	**GY**	52	46.4	43	38.4	73	65.2
	GI	60	53.6	69	61.6	39	34.8

Supplementary Document

Supplementary Notes

Supplementary Note 1: GI Patch-Corridor-Matrix

From a landscape ecology perspective, GI areas can be divided into patches, corridors (e.g., Waterway/Stream Corridor) and the background matrix (e.g., Urban) [9]. The patch-corridor-matrix model is one basic approach for understanding habitat diversity, functionality, and structural connectivity of GI networks [9,10], and these models have been widely utilized in research to map and understand the conditions of GI elements [11,12]. By mapping an existing GI network, the patch-corridor-matrix model helps researchers find areas where further improvement can enhance the quality and quantity of the network. This is a major focus of this study.

Several methodological process have been developed to model and map GI patches, hubs (core GI areas), and links between hubs or corridors over the matrix. Several studies have utilized graph theory [13], least cost analysis [14], kernel density methods [15], and morphological spatial pattern analysis (MSPA) to model and map patches and corridors and find functional and structural connectivity among landscape elements [12]. These models identify GI patches and links/corridors among these patches to explain existing GI networks. Exploring the connectivity and fragmentation of landscape elements can clearly identify GI assets and provide insights about how to improve and enhance them, which is a major consideration for MCC's 2015-2025 GI action plan [16].

Supplementary Note 2: ANN Details

Connected layers of artificial neurons mimic the information processing capacities of humans to solve problems. ANN's capacity to model complex and ambiguous relations, independent of statistical distribution, and its ability to use non-linearity make it a popular method in remote sensing, climate-science, land-use modelling [17]. ANN is broadly categorized into two classes: feed-forward networks (FFN), and recurrent networks (RN). FFN is used to solve static, non-recurrent processes. FFN maps inputs to set of outputs [18], only depicting forward moving connections [19,20]. Multilayer perceptron (MLP) is the most widely-used FFN method. Single layer perceptron is rarely used due to its limited processing capacity. Radial basis function nets (RBFN), are used with noised input and novel patterns. However, RBFN turn neurons are locally sensitive and less robust with classification and prediction problems. In contrast, MLP provides global generalization, effectively handles classification problems, and allows deep exploration of relationships between inputs [21,22].

MLP is used with supervised learning methods, with known input and outputs, and during the training of the network, node weights are adjusted based on error correction learning. MLP typically has three layers; input, hidden, output (Figure ANN1). Initially outputs are estimated using inputs and randomly assigned weights (*Wij*) within the nodes and activation functions at hidden (*Hj*) and output (*Ok*) nodes and adding random bias (Equation 1 and 2) [18].

$$\boldsymbol{Hj} = \boldsymbol{f^h}\left(\sum_{\boldsymbol{i=0}}^{\boldsymbol{p}} \boldsymbol{W_{ij}}\,\boldsymbol{X_i}\right) \ldots\ldots\ldots\ldots(\boldsymbol{Equation\ 1})$$

Where, *Hj* is the hidden node value of *ith* node; *Wij* is the randomly assigned weight between *Hj* and *Xi* node, and f^H is the activation Function (e.g., softmax, tanH)

$$\boldsymbol{Ok} = \boldsymbol{f^O}\left(\sum_{\boldsymbol{i=0}}^{\boldsymbol{p}} \boldsymbol{W_{jk}}\,\boldsymbol{H_j}\right) \ldots\ldots\ldots\ldots(\boldsymbol{Equation\ 2})$$

Where, *Ok* is the Output node value of *ith* node, *Wjk* is the randomly assigned weight between *Ok* and *Hj* node, and f^O is the activation Function (e.g., softmax, tanH)

Then, the network evaluates the estimated output against known outputs and calculates the error (Equation 3).

$$\boldsymbol{E_d} = \frac{\boldsymbol{1}}{\boldsymbol{2}}\sum_{\boldsymbol{k}}(\,\boldsymbol{\hat{z}_k}\,(\boldsymbol{d}) - \ \boldsymbol{O_k}\,(\boldsymbol{d})\,)^{\boldsymbol{2}} \ldots\ldots(\boldsymbol{Equation\ 3})$$

Here, $\hat{z}_k$(d) is the dth desired output in kth node, where the values are scaled to be commensurate with the given limit of selected activation function. Ed is the Error function on the dth input or output condition. In this case, the error have to be minimized, where the desired values tells the function what the output should be [23,18].

Using a gradient descent (GD) optimization process (Equation 4 and 5), error is *Back Propagated (BP)* in the network to update weights (Equation 6 and 7, Appendix C) using error value and estimated node outputs [23]. This process repeats until minimum error (Root means square error-RMSE, Means Square Error-MSE) is obtained between estimated output and desired output (known) values or a maximum number of iterations is achieved [22].

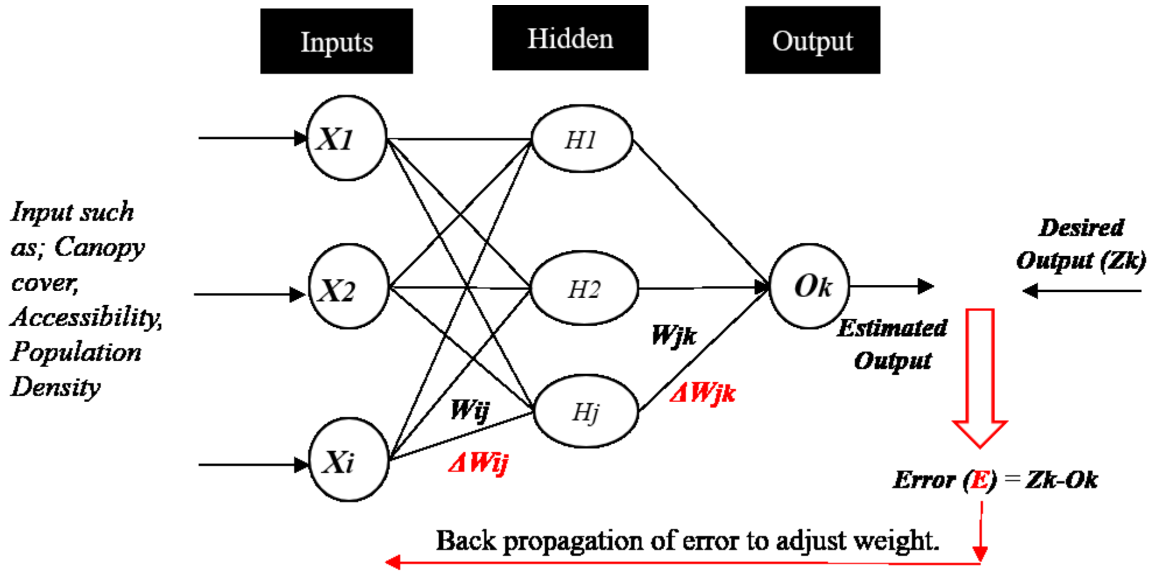

Figure ANN1: Typical structure and process of MLP. Input (*X*), forward weight (*W*), hidden neurons (*H*), output (*O*), adjusted weights (*ΔW*) based on error (*E*).

In addition to error and optimization, activation functions are vital to ANN performance. Activation functions are mathematical equations that transform computed values of a node/neuron within a given range (e.g., -1 to 1) [20]. This makes the signal clearer for following nodes. There are several activation functions available in areas of machine learning, including sigmoid, tanH, softmax [24, 25]. Sigmoid function transforms values between 0-1; tanH transforms values between -1 to 1; softmax computes values between 0-1 but has a slightly different calculation process compared to sigmoid and is better suited to prediction problems. Though selection of activation function is experimental based on data, tanH, softmax and ReLU are more popular than sigmoid functions due to their better performance with GD optimization [26].

Supplementary Figures

Supplementary Figure 1

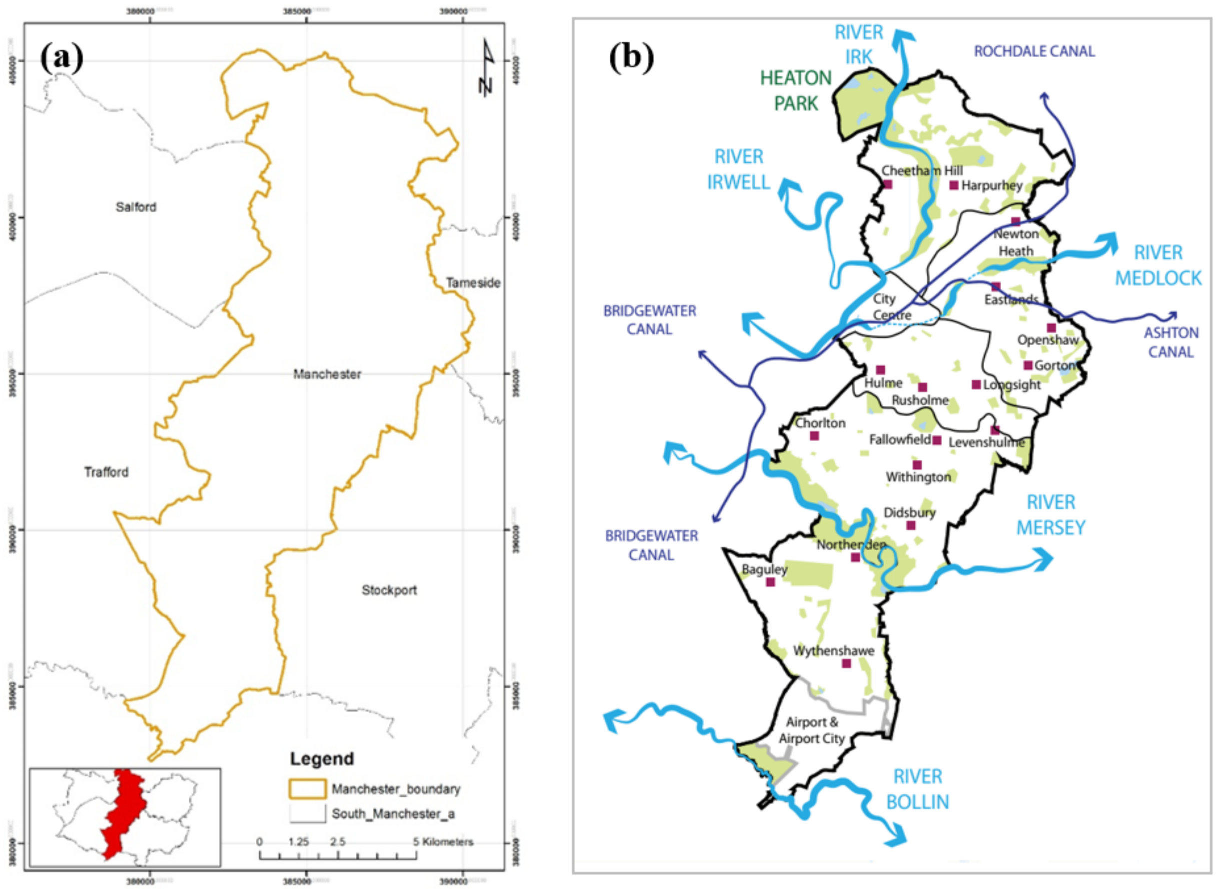

Supplementary Figure 1S: Study Area. (a) Geographic location and boundary of MCC (b) Important areas, river and canal network within study area [Source: 16]

Supplementary Figure 2S

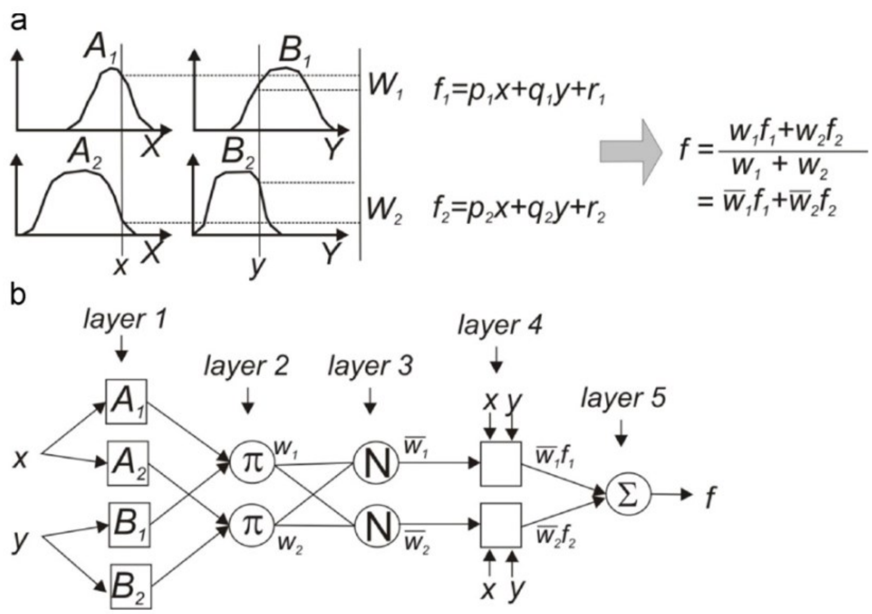

Supplementary Figure 3S: ANFIS Structure. (a) Tagaki and Sugeno fuzzy reasoning (b) ANFIS layers (Source: Jang, 1993)

Supplementary Figure 3S

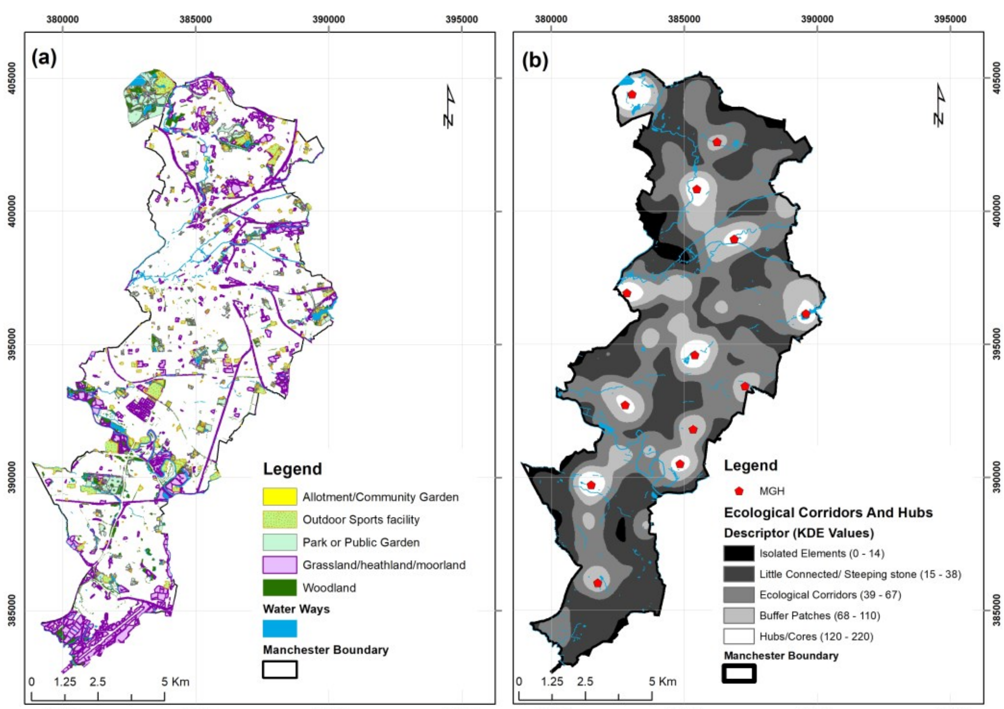

Supplementary Figure 4S: KDE Analysis results (a) GI elements considered for KDE (b) KDE surface indicating hubs and corridors.

Supplementary Figure 4S

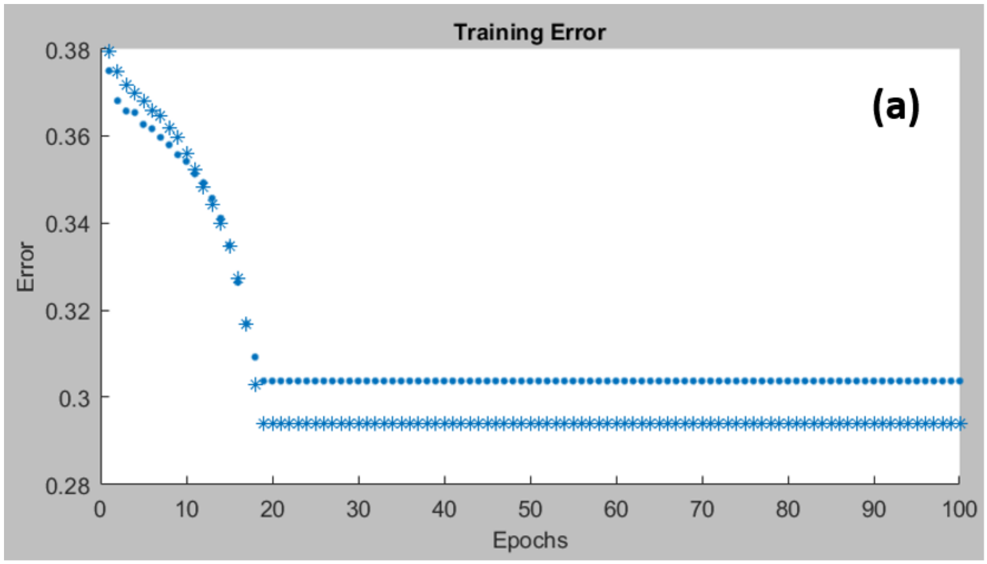

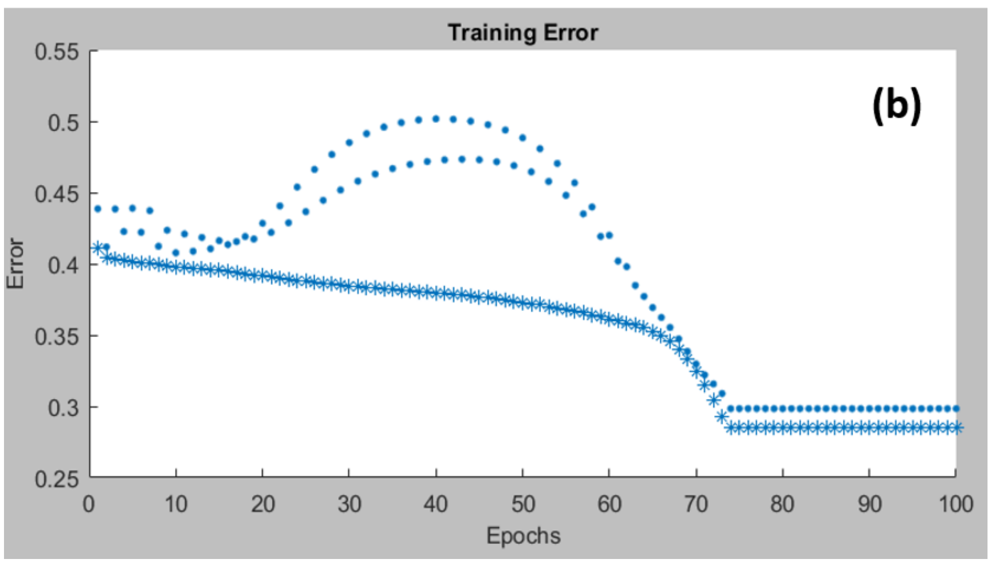

Supplementary Figure 4S: (a) Blue-stars indicate training data, blue-dots indicate test and validation data. As training and validation datasets were similar to the training set, it was concluded that the model trained better without overfitting. (b) The training error was much lower than validation and test errors (blue dots). At the beginning of training, the differences were higher; however, at the minimum error level, all errors become close, with no sign of overfitting.

Supplementary Figure 5S

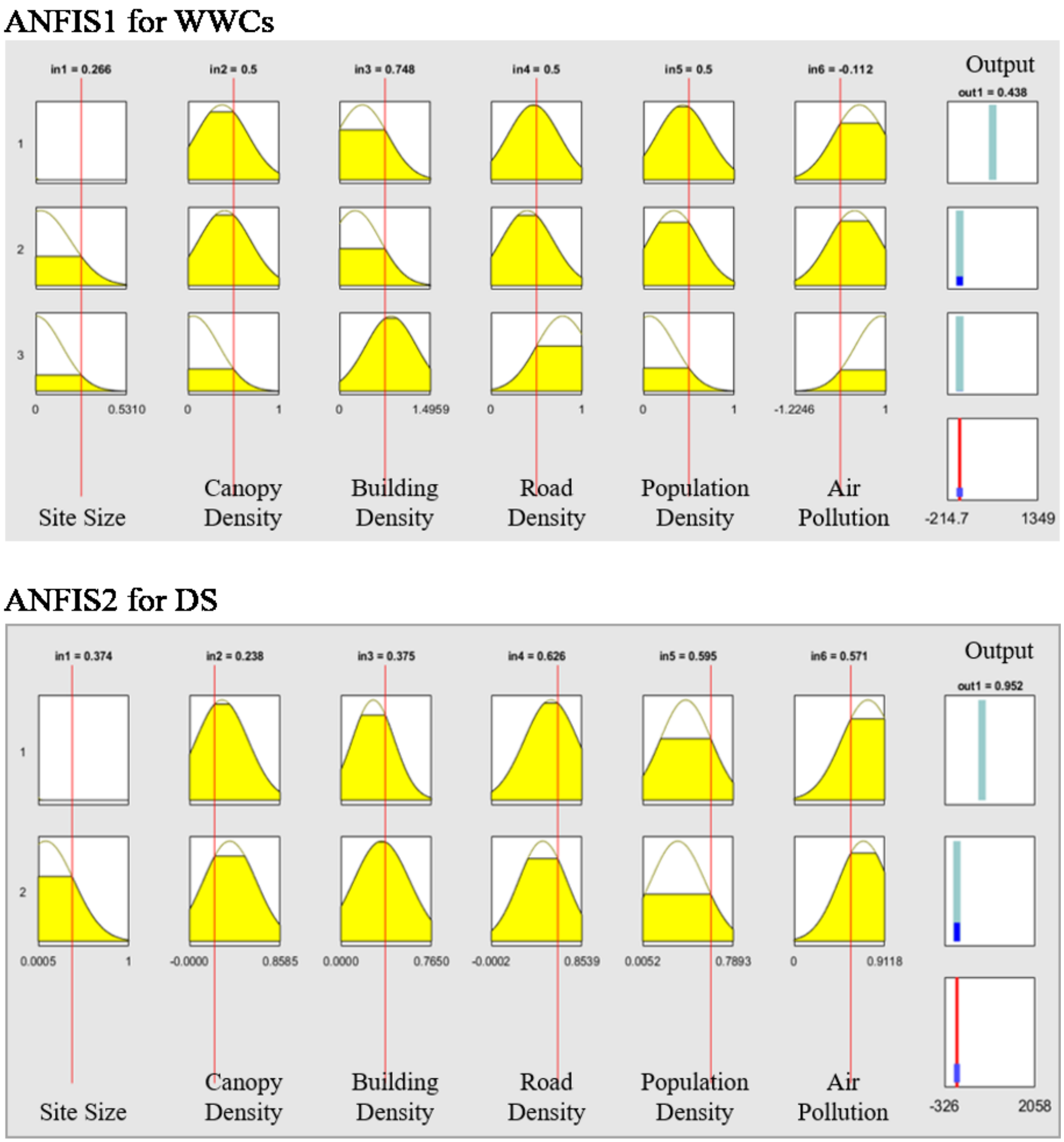

Supplementary Figure 8S: (a) Tuned MF of input variables generate rules for WWCs and their corresponding output values. (b) Tuned MF of input variables generate rules for DS and their corresponding output values

Supplementary Tables

Supplementary Table 1S: Five category of likelihood prediction for GI or GY transformation for the intervention types

Model Dataset	Model Type	Likelihood Prediction	Frequency	Percent
Water Way Corridors (WWCs)	**ANN_WWC**	Very low	14	9.3
		Low	9	6.0
		Medium	12	8.0
		High	22	14.7
		Very High	93	62.0
		Total	150	100.0
	ANFIS1_WWC	Very low	5	3.3
		Low	20	13.3
		Medium	21	14.0
		High	61	40.7
		Very High	43	28.7
		Total	150	100.0
	BL_WWC	Very low	7	4.7
		Low	22	14.7
		Medium	18	12.0
		High	15	10.0
		Very High	88	58.7
		Total	150	100.0
Derelict Sites	**ANN_DS**	Very low	41	36.6
		Low	5	4.5
		Medium	10	8.9
		High	17	15.2
		Very High	39	34.8
		Total	112	100.0
	ANFIS2_DS	Very low	17	15.2
		Low	18	16.1
		Medium	18	16.1
		High	23	20.5
		Very High	36	32.1
		Total	112	100.0
	BL_DS	Very low	29	25.9
		Low	31	27.7
		Medium	17	15.2
		High	13	11.6
		Very High	22	19.6
		Total	112	100.0

Supplementary Table 2S: LR classification accuracy for WWC and DS sites

Model Dataset	Observed		Predicted		
			GI/GY		Percentage Correct (%)
			GY	GI	
WWCs	GI/GY	GY	2828	79	97.3
		GI	630	379	37.6
	Overall Percentage				81.9
Derelict Sites	GI/GY	GY	385	57	87.1
		GI	94	330	77.8
	Overall Percentage (%)				82.6
The cut value is 0.5					

Supplementary Code Blocks

***Code Block 1:* Trained and tested MATLAB FIS file for ANFIS 1.** If just copy and paste in a text editor and save as *ANFIS1.FIS*, it can be usable in MATLAB for making prediction of similar type of sites for Current training.

```
[System]
Name='ANFIS1-WWC'
Type='sugeno' %FIS type
Version=2.0
NumInputs=6 %Independent Variables
NumOutputs=1 %Dependent Variable

NumRules=3
AndMethod='prod' %Rule methods
OrMethod='probor'

ImpMethod='prod'  % Scale the consequent membership function by the antecedent result value.

AggMethod='max'
DefuzzMethod='wtaver'  %Defuzzification Weighted average of all rule outputs.
[Input1]
Name='in1'
Range=[0 0.531005109]
NumMFs=3
MF1='in1cluster1':'gaussmf',[0.022547509352171  -0.0625857044850951]  # gaussmf, is Gaussian MF
MF2='in1cluster2':'gaussmf',[0.172608113272733 0.0271004387258185]
MF3='in1cluster3':'gaussmf',[0.152481406722877 0.00285529526774668]
[Input2]
```

```
Name='in2'
Range=[0 1]
NumMFs=3
MF1='in2cluster1':'gaussmf',[0.286337198775109 0.371536603164294]
MF2='in2cluster2':'gaussmf',[0.284082942968091 0.40019963798412]
MF3='in2cluster3':'gaussmf',[0.283618415568535 0.0579616244241595]
[Input3]
Name='in3'
Range=[0 1.47252015]
NumMFs=3
MF1='in3cluster1':'gaussmf',[0.420246539270456 0.370424335575643]
MF2='in3cluster2':'gaussmf',[0.412446164348133 0.257262374311394]
MF3='in3cluster3':'gaussmf',[0.416852521642308 0.845532587641545]
[Input4]
Name='in4'
Range=[0 1]
NumMFs=3
MF1='in4cluster1':'gaussmf',[0.282930478193309 0.467943417745509]
MF2='in4cluster2':'gaussmf',[0.281666279617729 0.397083561145775]
MF3='in4cluster3':'gaussmf',[0.285035758360276 0.786628996215121]
[Input5]
Name='in5'
Range=[0 0.995835006]
NumMFs=3
MF1='in5cluster1':'gaussmf',[0.281310226545579 0.434763130584271]
MF2='in5cluster2':'gaussmf',[0.282733957486755 0.334736652444195]
MF3='in5cluster3':'gaussmf',[0.282997542558149 0.0668310762846815]
[Input6]
Name='in6'
Range=[-1.22458559 1]
NumMFs=3
MF1='in6cluster1':'gaussmf',[0.63085083870651 0.358547032596929]
MF2='in6cluster2':'gaussmf',[0.627633310135066 0.234314870171436]
MF3='in6cluster3':'gaussmf',[0.629456221776336 0.888647230862715]
[Output1]
Name='out1'
Range=[0 1]
NumMFs=3
MF1='out1cluster1':'linear',[2100.79746722515 -20.1031903959326
55.7761277820974 -4.03603079616598 48.744876677239 25.5783357910766 -
88.6938991845938]
MF2='out1cluster2':'linear',[-1.25093547290195 0.169994949507728 -
1.09868125212805 0.928600574415855 -0.0319578264308482 -
0.228911893256694 1.0423861809898]
MF3='out1cluster3':'linear',[-1.10735960156442 1.66662895426365
0.115965385763757 -0.0018446389719328 -0.325158419549936
0.0188544140705525 -0.105921439873358]

[Rules]#Rule Sets
1 1 1 1 1 1, 1 (1) : 1
```

```
2 2 2 2 2 2, 2 (1) : 1
3 3 3 3 3 3, 3 (1) : 1
```

Code Block 2: **Trained and tested MATLAB FIS file for ANFIS 2.** If just copy and paste in a text editor and save as *ANFIS2.FIS*, it can be usable in MATLAB for making prediction of similar type of sites for Current training.

```
[System]
Name='ANFIS2-DS'
Type='sugeno' %FIS type
Version=2.0
NumInputs=6 %Independent Variables
NumOutputs=1 %Dependent Variable

NumRules=2

AndMethod='prod'
OrMethod='probor'
ImpMethod='prod'
AggMethod='max'
DefuzzMethod='wtaver'

[Input1]
Name='in1'
Range=[0.000527521 1]
NumMFs=2
MF1='in1cluster1':'gaussmf',[0.0488735343833279 -0.124509890495009]
MF2='in1cluster2':'gaussmf',[0.302009064135349 0.0795120211840388]

[Input2]
Name='in2'
Range=[-1.68861e-05 0.858521047]
NumMFs=2
MF1='in2cluster1':'gaussmf',[0.236832902184097 0.308919781872127]
MF2='in2cluster2':'gaussmf',[0.241169648911475 0.380237248165708]

[Input3]
Name='in3'
Range=[4.02048e-06 0.764984982]
NumMFs=2
MF1='in3cluster1':'gaussmf',[0.172367443013164 0.277606433954178]
MF2='in3cluster2':'gaussmf',[0.228259216809733 0.342141184496721]

[Input4]
Name='in4'
Range=[-0.000196786 0.853943402]
NumMFs=2
MF1='in4cluster1':'gaussmf',[0.241835951845382 0.559412296865533]
```

```
MF2='in4cluster2':'gaussmf',[0.220626871631596 0.487180964125005]

[Input5]
Name='in5'
Range=[0.005188638 0.789282548]
NumMFs=2
MF1='in5cluster1':'gaussmf',[0.212973322974857 0.374435487726315]
MF2='in5cluster2':'gaussmf',[0.223944482975753 0.310806384837631]

[Input6]
Name='in6'
Range=[0 0.911774435]
NumMFs=2
MF1='in6cluster1':'gaussmf',[0.256740562332863 0.741878509464578]
MF2='in6cluster2':'gaussmf',[0.239761524283577 0.698525903716989]

[Output1]
Name='out1'
Range=[0 1]
NumMFs=2
MF1='out1cluster1':'linear',[1627.32902813771    -31.2472159988958    -
20.9240453139163 13.2101357853083 35.2562561815911 38.0741737267595 -
51.8876444156971]
MF2='out1cluster2':'linear',[0.407278296062825    0.204639989288702    -
0.916774711347513      -0.0707611814070205      0.156307440666671     -
0.312938900163687 1.21644003393329]

[Rules]
1 1 1 1 1 1, 1 (1) : 1
2 2 2 2 2 2, 2 (1) : 1
```

Supplementary References

1. Allen III, W. L. (2012). Environmental Reviews And Case Studies: Advancing Green Infrastructure at All Scales: From Landscape to Site. *Environmental Practice*, *14*(1), 17-25. DOI: https://doi.org/10.1017/S1466046611000469

2. Mell, I. C., (2016). *Global Green Infrastructure: Lessons for successful policy-making, investment and management*. Routledge.

3. Sinnett, D., Smith, N. and Burgess, S. eds., (2015). *Handbook on Green Infrastructure: Planning, Design and Implementation*. Edward Elgar Publishing.

4. Tzoulas, K., Korpela, K., Venn, S., Yli-Pelkonen, V., Kaźmierczak, A., Niemela, J. and James, P., (2007). Promoting ecosystem and human health in urban areas using Green Infrastructure: A literature review. *Landscape and urban planning*, *81*(3), pp.167-178. DOI: https://doi.org/10.1016/j.landurbplan.2007.02.001

5. Kambites, C. and Owen, S., (2006). Renewed prospects for green infrastructure planning in the UK. *Planning, Practice & Research*, *21*(4), pp.483-496. DOI: 10.1080/02697450601173413

6. Burgess, S., (2015). Multifunctional green infrastructure: a typology. *Handbook on Green Infrastructure: Planning, Design and Implementation*, p.227.

7. Benedict, M.A. and McMahon, E.T., (2012). *Green infrastructure: linking landscapes and communities*. Island Press.

8. Mell, I.C., (2013). Can you tell a green field from a cold steel rail? Examining the "green" of Green Infrastructure development. *Local Environment*, *18*(2), pp.152-166. DOI: http://dx.doi.org/10.1080/13549839.2012.719019

9. Forman, R. T. (2014). *Land Mosaics: The Ecology of Landscapes and Regions (1995)* (p. 217). Island Press.

10. Forman, R.T., (1995). Some general principles of landscape and regional ecology. *Landscape ecology*, *10*(3), pp.133-142.

11. Dupras, J., Marull, J., Parcerisas, L., Coll, F., Gonzalez, A., Girard, M. and Tello, E., (2016). The impacts of urban sprawl on ecological connectivity in the Montréal Metropolitan Region. *Environmental Science & Policy*, *58*, pp.61-73. DOI: https://doi.org/10.1016/j.envsci.2016.01.005

12. Correa Ayram, C.A., Mendoza, M.E., Etter, A. and Salicrup, D.R.P., (2016). Habitat connectivity in biodiversity conservation: a review of recent studies and applications. *Progress in Physical Geography*, *40*(1), pp.7-37. DOI: 10.1177/0309133315598713

13. Minor, E.S. and Urban, D.L., (2008). A graph‐theory framework for evaluating landscape connectivity and conservation planning. *Conservation biology*, *22*(2), pp.297-307. DOI: 10.1111/j.1523-1739.2007.00871.x

14. Adriaensen, F., Chardon, J.P., De Blust, G., Swinnen, E., Villalba, S., Gulinck, H. and Matthysen, E., 2003. The application of 'least-cost 'modelling as a functional landscape model. *Landscape and urban planning*, *64*(4), pp.233-247. DOI: https://doi.org/10.1016/S0169-2046(02)00242-6

15. Biondi, E., Casavecchia, S., Pesaresi, S. and Zivkovic, L., (2012). Natura 2000 and the Pan-European Ecological Network: a new methodology for data integration. *Biodiversity and conservation*, *21*(7), pp.1741-1754. DOI: 10.1007/s10531-012-0273-7

16. MCC(Manchester City Council). (2018). Manchester's 'Green and Blue Infrastructure' strategy | 'Green and Blue Infrastructure' consultation | Manchester City Council. Available at: http://www.manchester.gov.uk/info/200024/consultations_and_surveys/6905/green_and_blue_infrastructure_consultation [Accessed 2 January 2018].

17. Mohammady, S., (2016). Optimization of adaptive neuro fuzzy inference system based urban growth model. *City, Territory and Architecture*, *3*(1), p.10. DOI: 10.1186/s40410-016-0039-8

18. Lee, S., An, H., Yu, S. and Oh, J.J., (2014). Creating an advanced backpropagation neural network toolbox within GIS software. *Environmental earth sciences*, *72*(8), pp.3111-3128. DOI: 10.1007/s12665-014-3216-7

19. Jain, A.K., Mao, J. and Mohiuddin, K.M., (1996). Artificial neural networks: A tutorial. *Computer*, *29*(3), pp.31-44.

20. Hornik, K., Stinchcombe, M. and White, H., (1989). Multilayer feedforward networks are universal approximators. *Neural networks*, *2*(5), pp.359-366.

21. Xie, T., Yu, H. and Wilamowski, B., (2011). Comparison between traditional neural networks and radial basis function networks. In *Industrial Electronics (ISIE), 2011 IEEE International Symposium on* (pp. 1194-1199). IEEE. DOI: 10.1109/ISIE.2011.5984328

22. Kecman, V., (2001). *Learning and soft computing: support vector machines, neural networks, and fuzzy logic models*. MIT press.

23. LeCun, Y., Bengio, Y. and Hinton, G., (2015). Deep learning. *Nature*, *521*(7553), pp.436-444. DOI:10.1038/nature14539

24. Suparta, W. and Alhasa, K.M., (2016). Adaptive neuro-fuzzy interference system. In *Modeling of Tropospheric Delays Using ANFIS* (pp. 5-18). Springer International Publishing.

25. Tang, Y., (2013). Deep learning using linear support vector machines. *arXiv preprint arXiv:1306.0239*.

26. Njikam, A.N.S. and Zhao, H., (2016). A novel activation function for multilayer feed-forward neural networks. *Applied Intelligence*, *45*(1), pp.75-82. DOI: 10.1007/s10489-015-0744-0